

AD621127

CEX-62.50

OPERATION BREN

NEUTRON-FIELD AND INDUCED-ACTIVITY
MEASUREMENTS—OPERATION BREN

F. M. Tomnovec and J. M. Ferguson

SEP 28 1965

CLEARING HOUSE
FOR FEDERAL AGENCY
TECHNICAL INFORMATION
hardcopy Microfilm
05.0 44 00
AEC

LIBRARY
TISA B

Issuance Date: September 1965

**CIVIL EFFECTS TEST OPERATIONS
U.S. ATOMIC ENERGY COMMISSION**

LEGAL NOTICE

This report was prepared as an account of Government sponsored work. Neither the United States, nor the Commission, nor any person acting on behalf of the Commission:

A. Makes any warranty or representation, expressed or implied, with respect to the accuracy, completeness, or usefulness of the information contained in this report, or that the use of any information, apparatus, method, or process disclosed in this report may not infringe privately owned rights; or

B. Assumes any liabilities with respect to the use of, or for damages resulting from the use of any information, apparatus, method, or process disclosed in this report.

As used in the above, "person acting on behalf of the Commission" includes any employee or contractor of the Commission, or employee of such contractor, to the extent that such employee or contractor of the Commission, or employee of such contractor prepares, disseminates, or provides access to, any information pursuant to his employment or contract with the Commission, or his employment with such contractor.

Printed in USA. Price \$1.00. Available from the Clearinghouse for Federal Scientific and Technical Information, National Bureau of Standards, U. S. Department of Commerce, Springfield, Va.

BLANK PAGE

NEUTRON-FIELD AND INDUCED-ACTIVITY MEASUREMENTS-OPERATION BREN

By

F. M. Tomnovec and J. M. Ferguson

Approved by: L. J. DEAL

Chief, Civil Effects Branch

Division of Biology and Medicine

**Naval Radiological Defense Laboratory
San Francisco, California**

NOTICE

This report is published in the interest of providing information which may prove of value to the reader in his study of effects data derived principally from nuclear weapons tests and from experiments designed to duplicate various characteristics of nuclear weapons.

This document is based on information available at the time of preparation which may have subsequently been expanded and re-evaluated. Also, in preparing this report for publication, some classified material may have been removed. Users are cautioned to avoid interpretations and conclusions based on unknown or incomplete data.

ABSTRACT

Operation BREN (Bare Reactor Experiment, Nevada) was an experiment that used a 1500-ft tower and a bare (no shielding) fast nuclear reactor patterned on "Godiva" to simulate a nuclear weapon detonated at various heights above the ground. Certain characteristics of the neutron field from this unshielded reactor were measured. The activation of gold, manganese, sulfur, cadmium-covered gold, and cadmium-covered manganese was determined as a function of distance from the reactor and of depth in the ground. The data show how those parameters, important for calculating neutron-induced activity in the soil, vary as a function of the height of the source and the slant range from the source.

ACKNOWLEDGMENTS

The authors gratefully acknowledge the following persons who gave assistance in Operation BREN and in the preparation of this report.

J. A. Auxier, Technical Director, F. W. Sanders, Deputy Technical Director, and F. F. Haywood, Oak Ridge National Laboratory, who assisted the authors during the many months of data taking.

W. H. Buser and E. W. Jones, Naval Radiological Defense Laboratory, preparation and experimental arrangements.

R. A. Taylor and R. F. Ehat, Naval Radiological Defense Laboratory, electronics.

D. M. Weldon, Naval Radiological Defense Laboratory, data analyses.

LCDR G. W. Werner and P. A. Read, Naval Radiological Defense Laboratory, determinations of neutron flux above the sulfur threshold.

CONTENTS

ABSTRACT	5
ACKNOWLEDGMENTS	6
CHAPTER 1 INTRODUCTION	9
1.1 Background	9
1.2 Objectives	9
1.2.1 Measurements near Ground Zero	10
1.2.2 Epicadmium-neutron Activation	10
1.2.3 Effect of Source Altitude	10
CHAPTER 2 METHODS	11
2.1 Sample Irradiation	11
2.2 Measurement of Relative Activities	12
CHAPTER 3 RESULTS	21
3.1 Discussion of Experimental Results	23
3.2 Summary	24
3.3 Conclusions	25

ILLUSTRATIONS

CHAPTER 2 METHODS

2.1 View from the Tower Showing the BREN Experimental Area During the Last Phase of the Tower Construction	13
2.2 Type of Terrain Around the 100-yd Station	13
2.3 Type of Terrain Around the 150-yd Station	14
2.4 Type of Terrain Around the 200-yd Station	14
2.5 Type of Terrain Around the 250-yd Station	15
2.6 Type of Terrain Around the 300-yd Station	15
2.7 Soil from a Hole near the 100-yd Station	16
2.8 Soil from a Hole near the 300-yd Station	16
2.9 View of the ORNL Revetment Showing the Strata That Are Usually Seen in This Area	17
2.10 Drill and Auger Used to Place the "Sabers" in the Ground	17
2.11 NRDL Personnel Drilling Holes with the Auger and Inserting Saber Sheaths into the Ground	18
2.12 Samples and Sample Holders for the Irradiation	18
2.13 Pulse-height Spectrum of ⁵⁶ Mn	19

ILLUSTRATIONS (Continued)

2.14 Method of Obtaining the Activity from the Pulse-height Spectrum	19
2.15 Efficiency Curve for the Gamma-ray Spectrometer	20

CHAPTER 3 RESULTS

3.1 Relative Gold Thermal-neutron Activation as a Function of Depth	26
3.2 Gold Epithermal Activations Vs. Depth	27
3.3 Gold Thermal Activation Vs. Depth, Normalized at the Surface	28
3.4 Gold Epithermal Activation Vs. Depth, Normalized at the Surface	29
3.5 Gold Thermal Activation Vs. Depth, Normalized at the Surface	31
3.6 Gold Epithermal Activation Vs. Depth, Normalized at the Surface	32
3.7 Gold Thermal Activation Vs. Depth for the 100-yd Station and 27-ft Reactor Height	34
3.8 Soil Moisture Content Vs. Time	34
3.9 Surface Gold Activation Vs. Slant Range	35
3.10 Manganese Activation Vs. Depth	35
3.11 Manganese Epithermal Activation Vs. Depth	37
3.12 Manganese Activation Vs. Depth	38
3.13 Manganese Epithermal Activation Vs. Depth	40
3.14 Sulfur Neutron Activation	41
3.15 Activation of Manganese, Copper, and Arsenic	42

TABLES

CHAPTER 2 METHODS

2.1 Properties of Induced Activities	12
--	----

CHAPTER 3 RESULTS

3.1 Density Measurements (g/cm^3)	21
3.2 Precipitation Recorded at Yucca Valley	22
3.3 Calculated Roentgens per Hour at Each Station and Reactor Height for a Given Sulfur Flux and Amount of Manganese in the Soil at Each Station	23
3.4 Percentage of the Total Radiation Field That Is Contributed by Manganese Activated by Neutrons Above the Cadmium Cutoff Energy	24

Chapter 1

INTRODUCTION

1.1 BACKGROUND

In airbursts of nuclear weapons, neutron-induced activity in the soil is one of the major residual hazards. The U. S. Naval Radiological Defense Laboratory (NRDL) has a continuing program for the study of this hazard. At Operation Teapot (1955), samples of different soils were exposed to nuclear weapon radiations and studied for the type and intensity of induced radioactivity.¹ For most soils, ^{28}Al , ^{56}Mn , and ^{24}Na are the dominating activities. Other activities may become important in unusual types of soil.

So that the dose rates from the induced activity can be predicted, certain measurements must be made near the ground-air interface. First, it is necessary to know the neutron-flux intensity and energy spectrum as a function of distance from Ground Zero and of depth in the ground. Second, it is necessary to know the effective neutron-activation cross sections of the important soil elements. These cross sections can be computed if the field neutron-energy spectrum is well known and if the activation cross sections have been measured as a function of energy for each element. However, these quantities generally are not known, and thus field measurements are necessary.

At Operation Plumbbob in 1957, NRDL undertook the measurement of some of these quantities.² Samples of the important soil elements were placed in an array at various distances and depths around nuclear airbursts. The specific activities of about 30 different elements were determined with a gamma-ray spectrometer. The neutron flux over various energy ranges was measured by using gold, cadmium-covered gold, and sulfur threshold detectors. These data and a description of the measurements are given in Ref. 2, and an analysis of the data is given in Ref. 3.

In the period since 1957, these results have been supplemented by a series of laboratory experiments and calculations. This later work was directed toward the problem of applying the field results to conditions other than those at Operation Plumbbob. The information still had gaps. In particular, some questions remained about the activation of manganese by epithermal neutrons; there was little or no data concerning the neutron flux, neutron activation, or neutron-induced activity dose rates for the area within about 200 yd of Ground Zero; and there was little information about the effects of varying the burst height.

1.2 OBJECTIVES

The experimental technique used at Operation BREN was to simulate the neutron radiation field from a nuclear weapon with a reactor. The unshielded fast reactor [the Oak Ridge National Laboratory Health Physics Research Reactor (HPRR)] was raised in a hoist to various elevations on a 1500-ft tower. Measurements of dose rate by Program 1 were taken, in various configurations, inside facsimiles of Japanese houses typical of those in Hiroshima and Nagasaki in 1945. This study is to help evaluate the radiation doses received by persons exposed to nuclear weapons, especially the residents of Hiroshima and Nagasaki, Japan. Other

selected programs that could utilize the radiation fields available on a noninterference basis were included as parts of the operation.⁴

The general aim of Program 5 was to determine the neutron-energy spectrum and soil radioactivity resulting from a neutron source in the air as a function of distance from the source and of depth in the ground. Gold and sulfur activation data serve as measurements of the relative neutron flux, and the data on manganese give its relative effective activation cross section in the neutron field near the ground-air interface.

The reactions involved in this experiment are as follows:

$^{32}\text{S}(n,p)^{32}\text{P}$	Effective threshold is 3.0 Mev
$^{197}\text{Au}(n,\gamma)^{198}\text{Au}$	Thermal-neutron activated
$^{55}\text{Mn}(n,\gamma)^{56}\text{Mn}$	Thermal-neutron activated

The specific objectives of this program are described in Secs. 1.2.1 to 1.2.3, which follow.

1.2.1 Measurements near Ground Zero

In a nuclear blast it is difficult to expose and recover samples near Ground Zero since the samples must not be shielded from neutrons, and yet must withstand the blast and thermal radiation. On the other hand, this is the easiest region in which to make reactor measurements since it is close to the source. At BREN, therefore, particular emphasis was placed on getting data extending from close to the base of the tower to 200 yd away, since data for these distances could be normalized to weapons-test results.

1.2.2 Epicadmium-neutron Activation

The Plumbbob measurements² indicate that certain elements, notably manganese, are substantially activated by epicadmium neutrons³—neutrons with energies greater than about 0.3 ev. If the field data are used, it is hard to correlate this activation with the epicadmium flux since the thermal-neutron activation must be subtracted out. At BREN, both gold and manganese were cadmium shielded. Originally it was intended that similar measurements be made for sodium, copper, and arsenic. However, data for these elements were obtained only at the 30-yd station because the flux levels were too low.

1.2.3 Effect of Source Altitude

Most of the weapons-test data are for bursts at a 500-ft altitude. Since air absorption is important, a simple inverse-square correction cannot be used to extrapolate to other altitudes. Data on the activation at fixed positions in the soil and for a fixed type of source, but for different altitudes, should provide the information needed for altitude corrections.

REFERENCES

1. R. F. Johnson, C. S. Cook, L. A. Webb, and R. L. Mather, *Neutron-induced Radioactive Isotopes in Soil*, Project 2.3a, Operation Teapot, Report WT-1117, Aug. 7, 1958.
2. C. S. Cook, W. E. Thompson, F. M. Tomnovec, R. L. Mather, J. M. Ferguson, and P. R. Howland, *Neutron-induced Activities in Soil Elements (U)*, Project 2.2, Operation Plumbbob, Report WT-1411, July 31, 1959. (Classified)
3. R. L. Mather, *Neutron Energy Effects and Induced Activation (Plumbbob Observations)*, Report USNRDL-TR-465, Naval Radiological Defense Laboratory, Sept. 28, 1960. (Classified)
4. F. W. Sanders, F. F. Haywood, M. J. Lundin, L. W. Gilley, J. S. Cheka, and D. R. Ward, *Operation Plan and Hazards Report—Operation BREN*, USAEC Report CEX-62.02, April 1962.

Chapter 2

METHODS

The type of data needed is the relative activities of certain elements exposed at various distances from the reactor and at various depths in the ground. The discussion of experimental technique is divided into two parts: (1) the positioning and irradiation of the samples and (2) the determination of the relative activities of the irradiated samples.

2.1 SAMPLE IRRADIATION

Small samples of gold, sulfur, and manganese were placed in an array at various distances and depths around the reactor tower. The distances varied from 30 to 400 yd; the depths ranged from the surface to 20 in. under ground. The activity induced in the samples at the further stations often was too weak to measure. The greatest distance at which data were obtained was 400 yd. Figure 2.1 shows a view from the tower and the relation of the station array relative to the BREN experimental area.¹ Figures 2.2 to 2.6 show views of the stations and of the type of terrain at each station. The terrain varied from one station to another. Figures 2.7 and 2.8 show the difference in soil composition between the 100- and the 300-yd station, the 300-yd station indicating a rather large increase in rock content, especially in size. Figure 2.9 shows another view of the stratum effect which was noticed at the BREN area and which is common to this area. The total effect of this variation in soil composition was not noticeable in the final results.

At each distance "saber" type sample holders were put in the ground. Figure 2.10 shows the auger drill used to make holes in the soil which take the holders and some of the sample holders used in this experiment. Figure 2.11 shows personnel placing the sample holders into the ground. Each hole was filled with soil after the sample holder was in place. The "sheath" of the saber is a light aluminum tube of cylindrical or rectangular cross section, and the saber itself is a light piece of aluminum which holds the samples and which slides in and out of the sheath. After the sheaths had been placed in the ground, the samples were positioned or recovered by sliding the saber in or out. Figure 2.12 shows the sample holders and some of the samples.

The obvious question about this technique is whether the aluminum perturbs the neutron flux at the sample position. At Operation Plumbbob, most of the samples were suspended inside large dirt-filled canisters buried in the ground.² At some stations "sabers" were buried near the canisters for comparison. The differences between the saber results and the canister results were not systematic and were well within the experimental error.

An experimental run was made at the 60-in. cyclotron of the University of California by using the neutron source of protons on beryllium to investigate the moderating influence of aluminum sample holders on fast neutrons. Gold detectors established the thermal-neutron flux with the presence of the aluminum holders and without the aluminum. No observable effects were noticed. Calculations also show that the absorption of thermal neutrons by the aluminum holders is less than 1%. From Plumbbob data we have, for Nevada Test Site (NTS)

soil with a moisture content of 6%, a mean free path for sulfur neutrons of 5.1 in. Since the holders for the thermal-neutron detectors have $\frac{1}{4}$ in. of aluminum, thicknesses of about $\frac{1}{20}$ th of a mean free path are involved. We conclude that differences between aluminum and NTS soil are not sufficient to perturb the flux in this situation.

The gold and sulfur samples are disk shaped; their size and shape are determined by the counting technique described in Sec. 2.2. The manganese samples weigh 1 g each, and they are sealed in pharmaceutical gelatin pills. The gold and manganese samples were counted with a gamma-ray spectrometer. The thermal-neutron capture cross section of manganese is large enough that neutron attenuation in the sample must be corrected for; this correction factor has been determined in the laboratory.²

Cadmium covers were provided for both the gold and the manganese samples. A bare sample and a cadmium-covered sample were placed at each position. So that flux perturbation by the cadmium would be avoided, the two types of samples were kept well separated.

2.2 MEASUREMENT OF RELATIVE ACTIVITIES

The properties of the induced activities are given in Table 2.1. No samples of manganese were irradiated for more than one day because of its short half-life. The samples were put in position the day before irradiation and were recovered when the reactor was shut down for the day. They were then taken back to the NRDL mobile-laboratory trailer at Camp Mercury.

TABLE 2.1 — PROPERTIES OF INDUCED ACTIVITIES

Activity	Half-life	Activity counted
³² P (from sulfur)	14 days	Beta rays
⁵⁶ Mn	2.58 hr	0.845-Mev gamma
¹⁹⁸ Au	2.70 days	0.412-Mev gamma

The trailer contained a gamma-ray spectrometer, which was used to measure the activity in the manganese and gold samples. This spectrometer, which is basically the same as the one used at Plumbbob, consists of a 4-in.-high 4-in.-diameter NaI(Tl) crystal, a 100-channel analyzer, and the associated electronics. This equipment is described in Ref. 2. The sample to be measured is put in a holder which positions the sample 1 in. from the face of the crystal. Figure 2.13 shows a typical pulse-height spectrum taken with this apparatus.

The full-energy peak of the prominent gamma ray in each spectrum is used to determine the activity in the sample. The area under the peak is determined as shown in Fig. 2.14. The activity of the sample, in counts per second, is obtained from the area by using an empirical, energy-dependent correction factor (Fig. 2.15). In the determination of the relative activity of the sample at the end of the irradiation, the sample weight and the decay of the activity with time must also be corrected for. Reference 2 elaborates on this technique.

The sulfur activity was determined by beta-ray counting by using Geiger-Mueller tubes in a reproducible geometry. The factor for converting from counts to neutron flux is empirical and has been determined by intercomparison with other laboratories. The sulfur-measurement system was calibrated by using the 14-Mev neutron source at Los Alamos. The half-life of the ³²P is such that there was enough time to ship the samples back to NRDL for counting. As an alternative method when the neutron flux was low, the samples were ashed to increase the counting efficiency, and their activities were determined with a calibrated Geiger-Mueller counter mounted in a Baird-Atomic, Inc., model 750 automatic counting apparatus. Each counting system at any laboratory has to be calibrated in terms of the various parameters, detector size, thickness, geometry, etc.; therefore calibration data here are not presented since they are not pertinent to other laboratories.

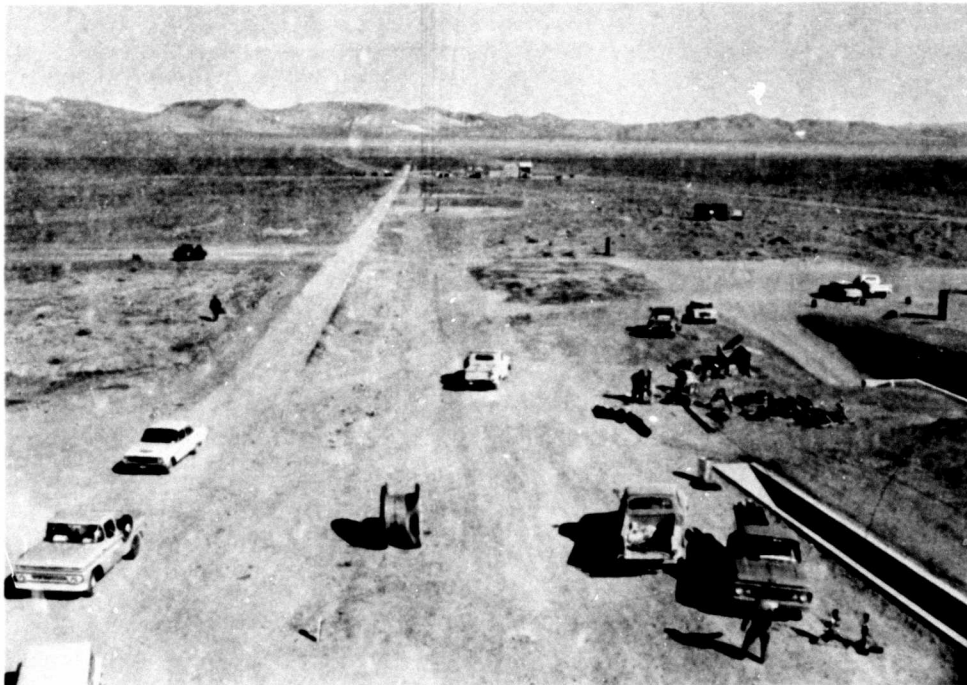


Fig. 2.1 — View from the tower showing the BREN experimental area during the last phase of the tower construction. The trailer of Program 4 is at the right background, the Japanese houses are visible in the background, and the induced-activity measuring stations of Program 5 are to the left of the road. Close scrutiny will show the flags indicating each station, starting with the 100-yd station. NRDL activity is visible at the 150-yd station.

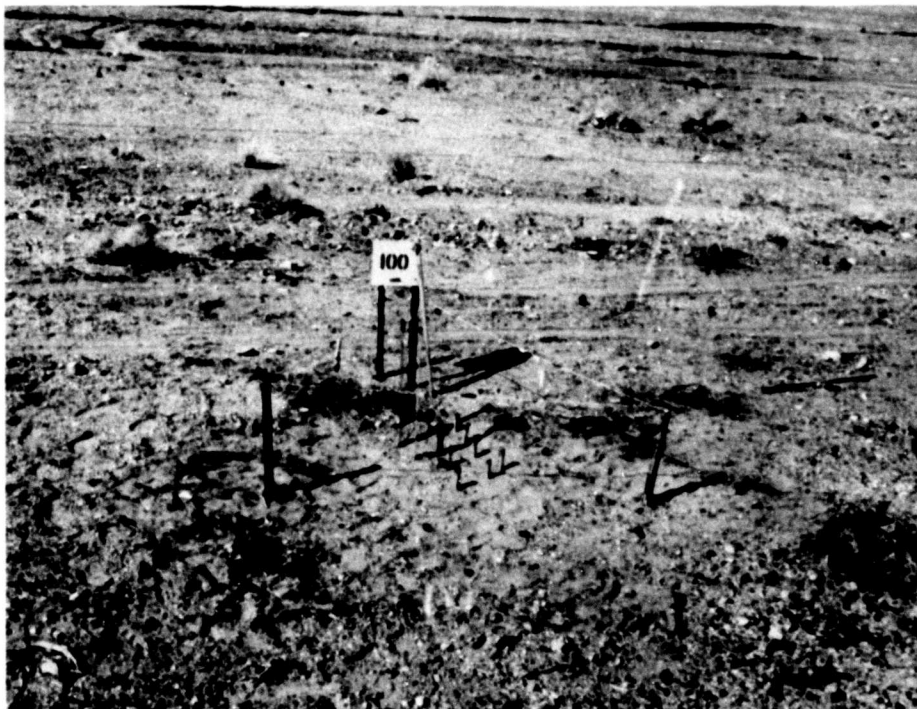


Fig. 2.2 — Type of terrain around the 100-yd station.



Fig. 2.3 — Type of terrain around the 150-yd station.

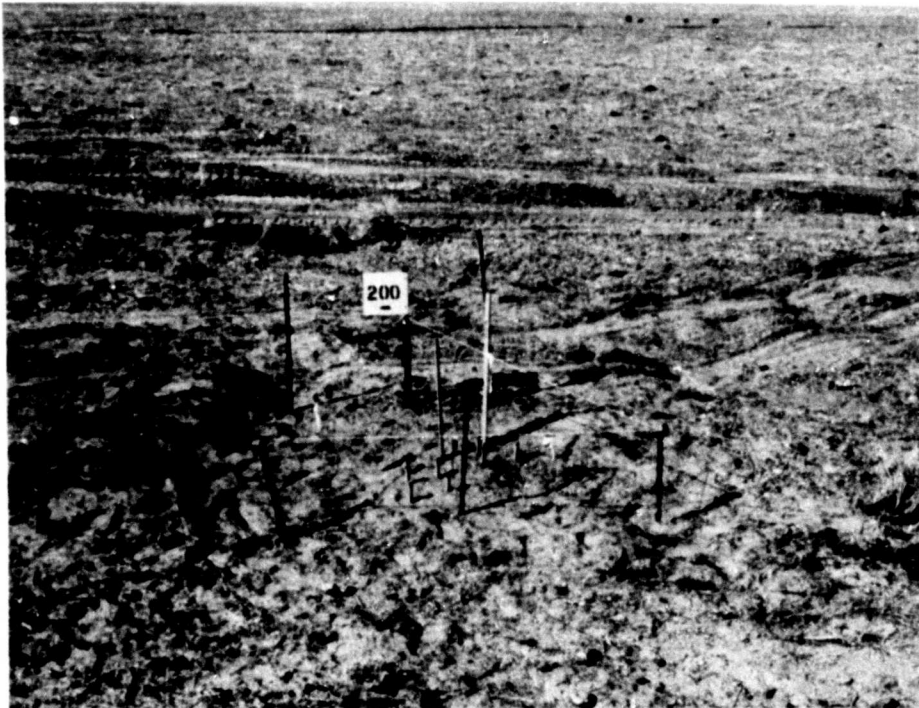


Fig. 2.4 — Type of terrain around the 200-yd station.

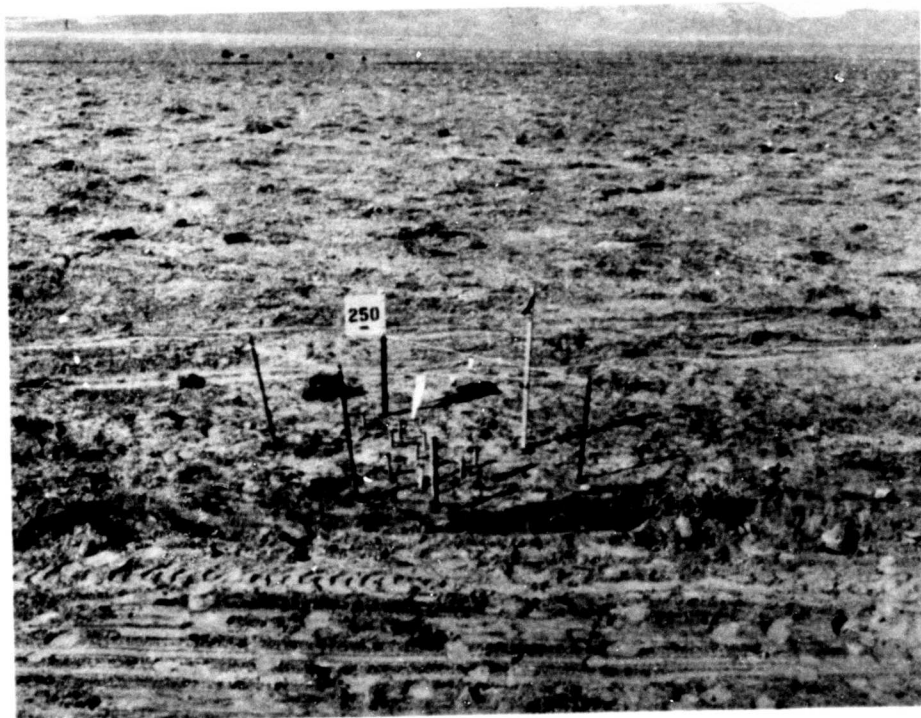


Fig. 2.5 — Type of terrain around the 250-yd station.

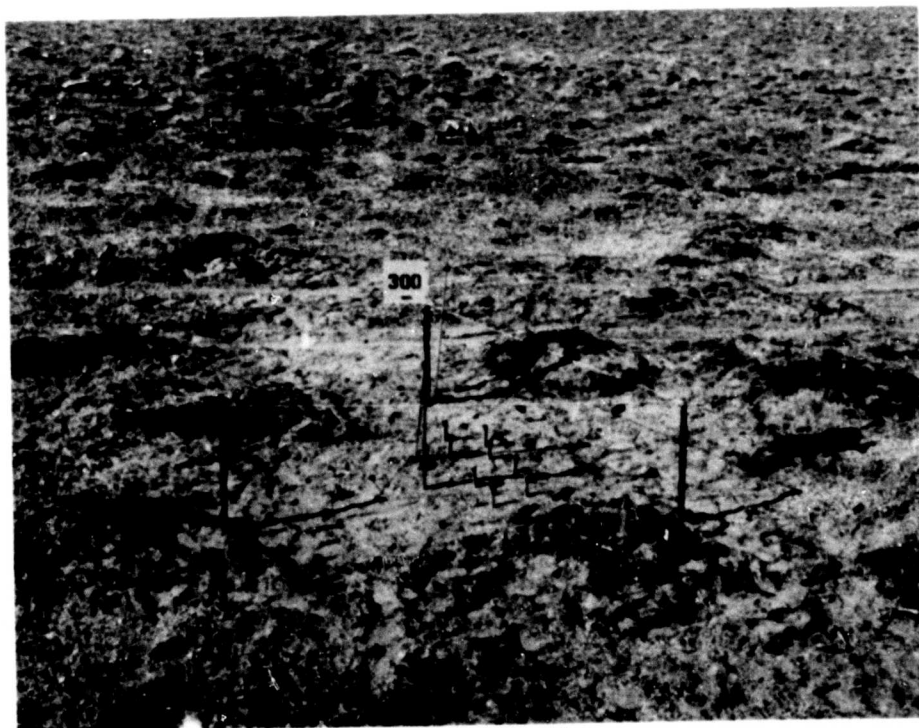


Fig. 2.6 — Type of terrain around the 300-yd station.

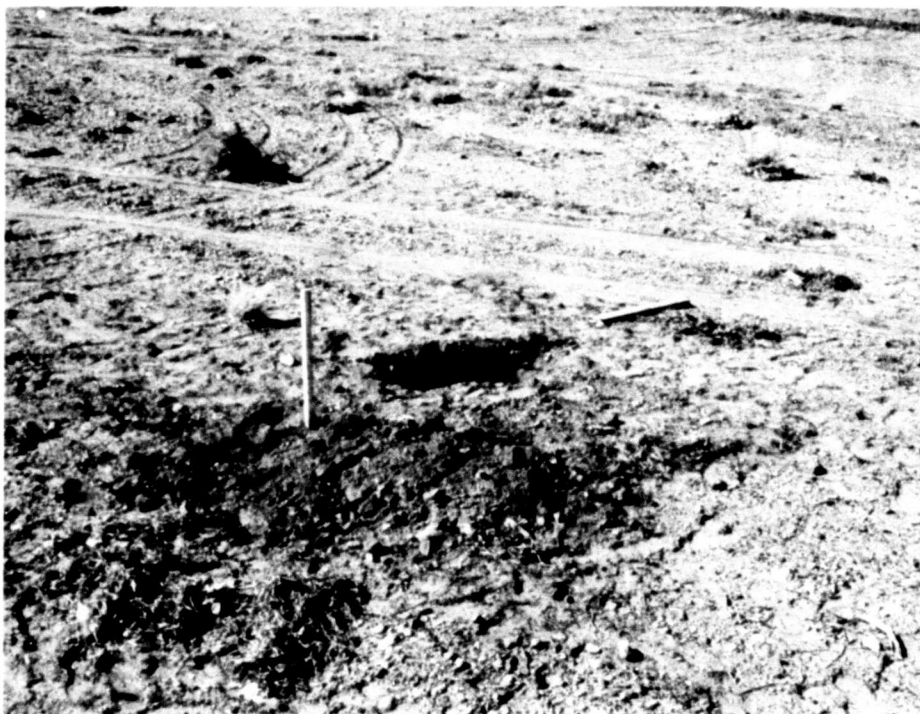


Fig. 2.7—Soil from a hole near the 100-yd station. The ground in this area is composed of small stones and soil.



Fig. 2.8—Soil from a hole near the 300-yd station. The ground at this point has many large stones.

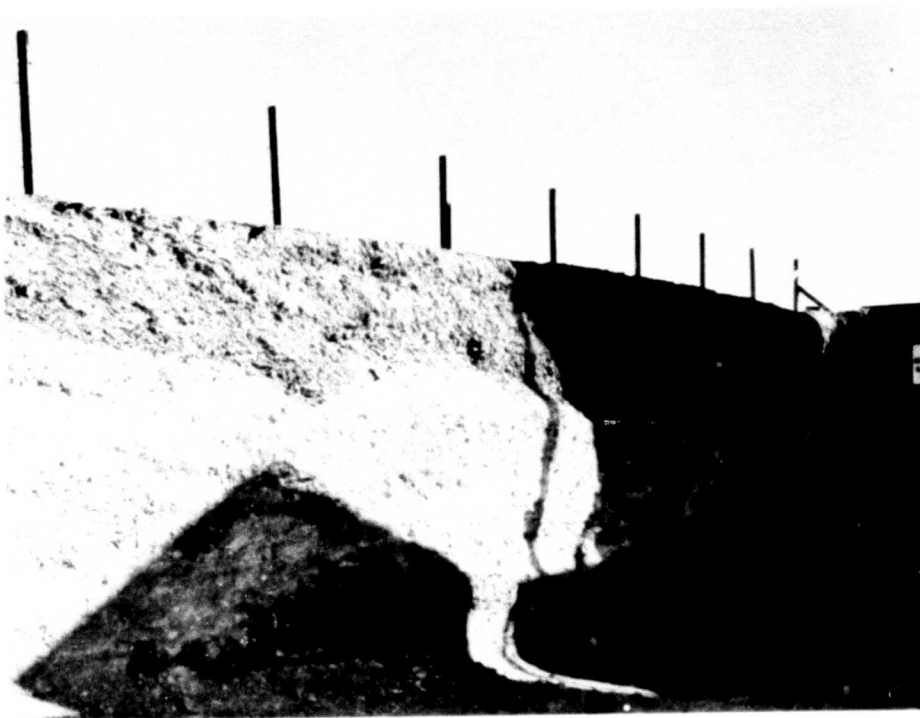


Fig. 2.9 — View of the ORNL revetment showing the strata that are usually seen in this area.

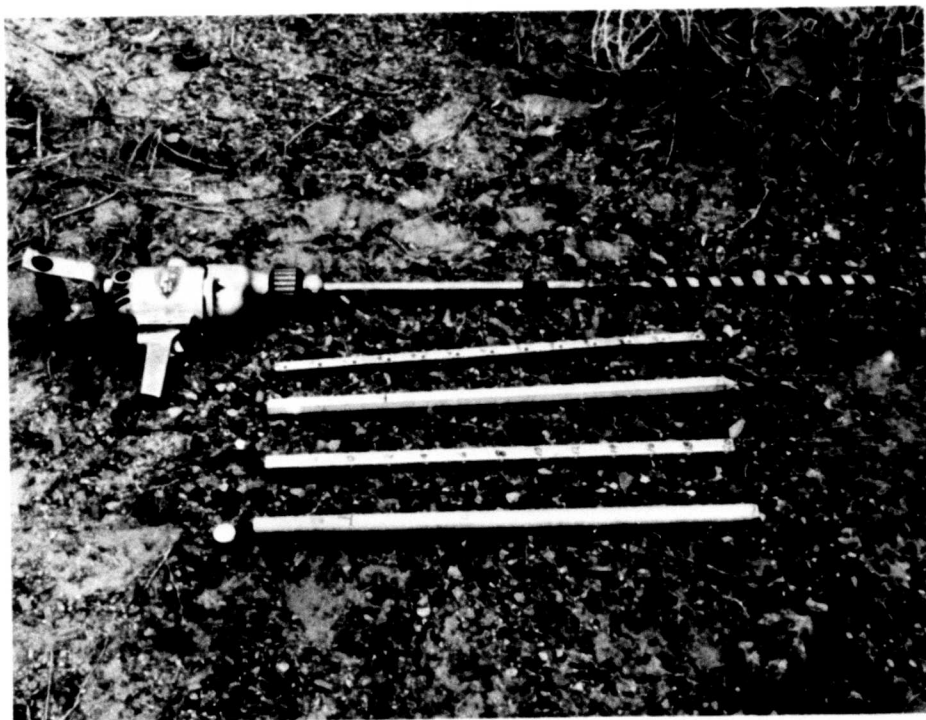


Fig. 2.10 — Drill and auger used to place the "sabers" in the ground. A gold and an element sample holder are shown.



Fig. 2.11 — NRDL personnel drilling holes with the auger and inserting saber sheaths into the ground.

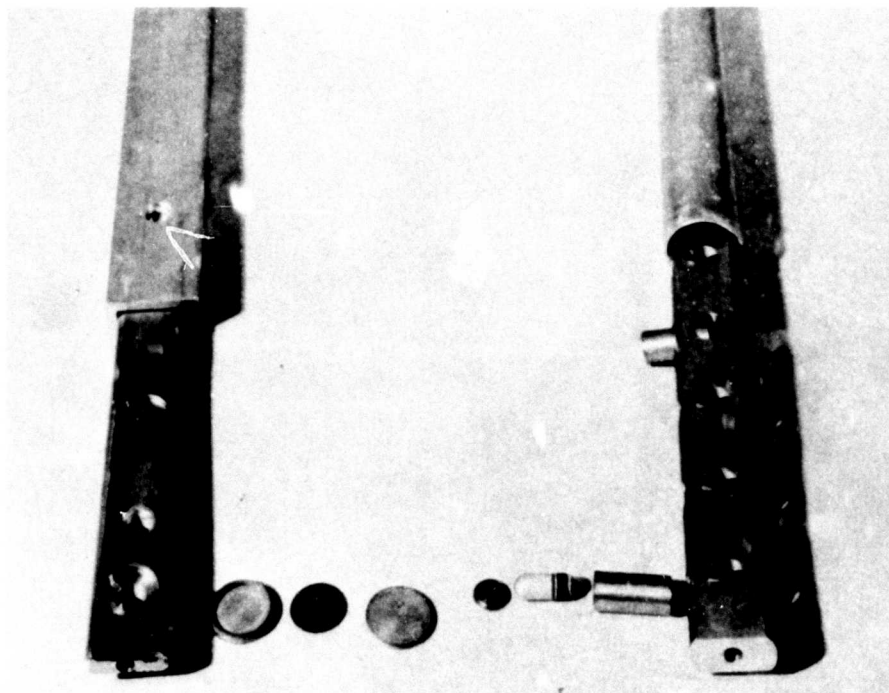


Fig. 2.12 — Samples and sample holders for the irradiation. On the left is a gold sample holder partially inserted in its sheath. The recesses for the top two samples are exposed. The next three items are a cadmium holder, a gold sample, and a cadmium lid. The three small items on the right are a cadmium lid, a sodium sample, and a cadmium holder for the sodium. On the right is a saber for positioning the sodium samples, partially inserted in its sheath.

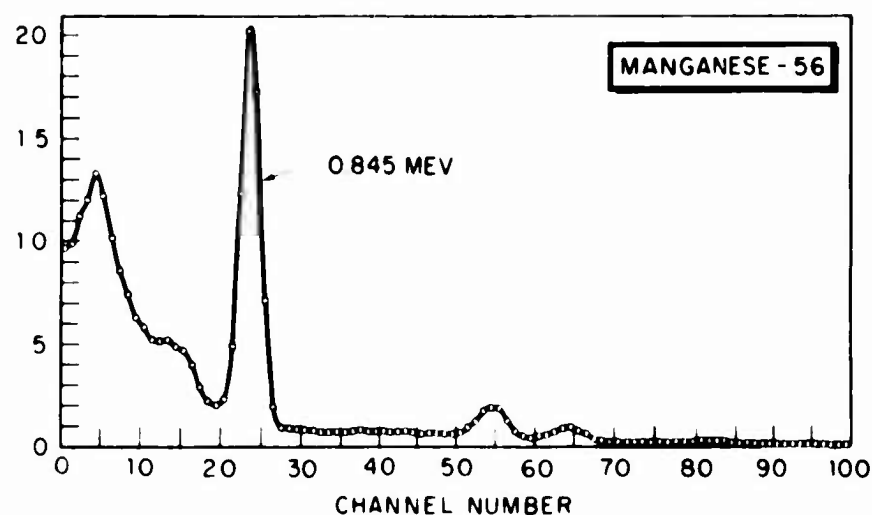


Fig. 2.13—Pulse-height spectrum of ^{56}Mn . This figure shows the ^{56}Mn gamma-ray pulse-height spectrum taken with the mobile-laboratory spectrometer. Counting rate is plotted against channel number (pulse height). The peaks at channels 24, 55, and 64 correspond to gamma rays with energies of 0.845, 1.8, and 2.1 Mev, respectively. The 0.845-Mev gamma-ray peak was used to determine the activity, as shown in Fig. 2.3.

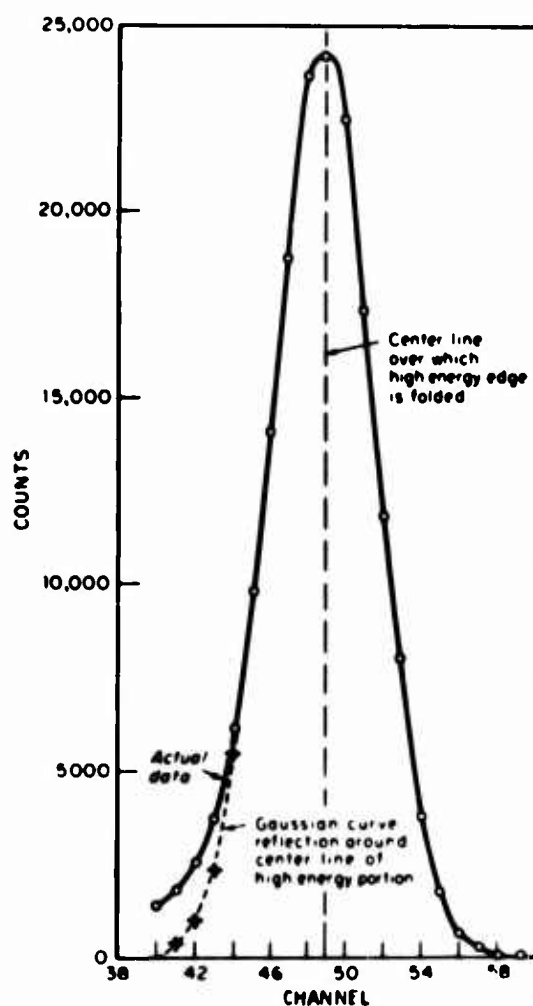


Fig. 2.14—Method of obtaining the activity from the pulse-height spectrum. The full-energy peaks in the pulse-height spectrum are well represented by a Gaussian curve. The curve is fitted to the high-energy side of the peak, and the area of the curve is proportional to the activity in the sample.

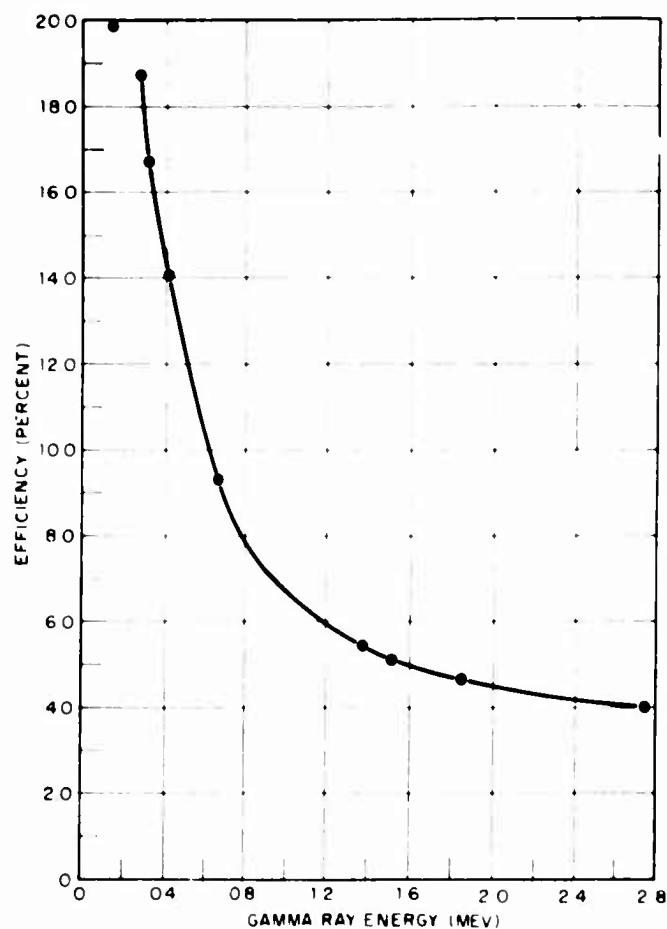


Fig. 2.15 — Efficiency curve for the gamma-ray spectrometer. The ordinate represents the percentage of photons emitted from the sample which will contribute to the full-energy peak of the pulse-height spectrum.

REFERENCES

1. F. W. Sanders, F. F. Haywood, M. I. Lundin, L. W. Gilley, J. S. Cheka, and D. R. Ward, *Operation Plan and Hazards — Operation BREN*, USAEC Report CEX-62.02, April 1962.
2. C. S. Cook, W. E. Thompson, F. M. Tomnovec, R. L. Mather, J. M. Ferguson, and P. R. Howland, *Neutron-induced Activities in Soil Elements (U)*, Project 2.2, Operation Plumbbob, Report WT-1411, July 31, 1959. (Classified)

Chapter 3

RESULTS

The results of the experiment are presented in Figs. 3.1 to 3.15. The relative activation of the samples is usually plotted vs. depth in the ground for each detector station. The curves labeled epithermal neutron activation represent the activities of cadmium-covered samples, and the data labeled thermal-neutron activation were obtained by subtracting the cadmium-covered activation from the activation of the bare samples.

The relative gold thermal-neutron activities at the different stations for four reactor heights are shown in Fig. 3.1. The probable error of each number is about 10%. Similar plots for the gold epithermal activity are shown in Fig. 3.2.

Figure 3.3 shows the same data as in Fig. 3.1, except that the curves are normalized at the surface for comparison of their shapes, showing the buildup of thermal-neutron flux in the ground. Figure 3.4 is the same type of plot for the gold epithermal activity.

In Fig. 3.5 the gold thermal flux is again normalized at the surface, but in this case each station is plotted separately, with varying reactor heights. Figure 3.6 is the corresponding curve for the gold epithermal flux.

It is evident from Figs. 3.1 to 3.6 that the neutron distribution in the ground is not a simple function of a few parameters. For a given station the shape changes with reactor height. For the same reactor height, the shape changes with the distance from the tower. Also, the data show that the shape should be sensitive to local variations in the soil density and composition as well as to the number of air mean free paths from the reactor. The soil density at each of the stations is given in Table 3.1.

TABLE 3.1 — DENSITY MEASUREMENTS (G/CM³)

Station (yards from tower base)	FMT*	WB*	JMF*	Average	Probable error	Probable range
30		2.02	1.96			
100	1.47	1.83	1.63	1.64	0.10	1.54 to 1.74
150	1.80	1.63	1.80	1.74	0.06	1.68 to 1.80
200	1.33	1.23	1.56	1.37	0.10	1.27 to 1.47
250	1.38	1.50	1.65	1.51	0.08	1.43 to 1.59
300	1.60	1.63	2.12	1.78	0.17	1.61 to 1.95
350	1.60	1.50	1.73	1.61	0.07	1.54 to 1.68
400	1.47	1.73	1.53	1.58	0.08	1.50 to 1.66
450	1.41	1.43	1.31	1.38	0.04	1.34 to 1.42
500	1.56	1.89	2.00	1.82	0.13	1.69 to 1.95

*Experimenter's initials.

A particularly interesting variable is the soil moisture content.⁵ The moderating properties of the soil depend critically on the moisture. The effect is shown in Fig. 3.1. These two sets of data were taken under identical conditions except that one set was taken later in the

year after the rain had stopped and the soil moisture content had dropped. The rainfall and soil-moisture variations for the data-taking period are given in Table 3.2 and Fig. 3.8. The curve for the drier soil shows less peaking and less rapid falloff with depth.²

TABLE 3.2 — PRECIPITATION RECORDED AT YUCCA VALLEY*

Date	Rain, in.	Snow, in.
January		
20	Trace	Trace
21	0.18	2 (on ground)
22	0.03	4 (on ground)
February		
7	Trace	
8	0.14	
9	0.01	
10	0.42	
11	0.28	
14	Trace	
15	0.02	
16	0.01	Trace
17	Trace	Trace
19	0.28	Trace
20	0.01	Trace
24		Trace
25		0.01 (water equiv.)
26		Trace
March		
6	0.08	
7	0.09 (with hail)	
9		0.02
11		Trace
20	Trace	
21	0.01	
22	0.04 (with hail)	
29	Trace	
May		
14	Trace	
15	0.01	
16	Trace	
27	Trace	
June		
1	Trace	

*These data were recorded at the weather station at the Yucca airstrip. The rainfall at the BREN tower site would have been somewhat different. However, the Yucca airstrip data should give a good indication of the amount of rain, or lack of it, at the BREN tower site.

Figure 3.9 shows the variation of the surface neutron flux (gold thermal and epithermal) with slant range from the reactor. The data roughly follow a smooth curve, but it is evident that, for a given slant range, the flux is not independent of reactor height.

The manganese data are given in Figs. 3.10 to 3.13. The manganese thermal flux follows the gold thermal flux well for a given set of conditions. However, manganese and gold runs taken for the same geometries but at different times of the year (which means different soil moisture) are not the same. The manganese epithermal and gold epithermal results also show about the same behavior, although the two elements are sensitive to somewhat different ranges of neutron energies.

Some fast-neutron data obtained by using sulfur threshold detectors are shown in Fig. 3.14.

One set of data was obtained for two other elements, copper and arsenic, at the 30-yd station and a reactor height of 27 ft. These elements were chosen because they are potentially important in the induced-activities problem and because they have high epithermal cross sections. The relative activities are shown in Fig. 3.15. No attempt was made to correct for the

various disintegration rates of the gamma ray chosen for each isotope. The absolute relation between each element from a given neutron flux is not presented here either but, rather, a comparison of the relative activity of each isotope as a function of depth in the ground; thus the shapes of the curves show the differences that can be attributed to the different energy variations of the activation cross sections.

3.1 DISCUSSION OF EXPERIMENTAL RESULTS

The manganese data were normalized to the surface-activated manganese. These manganese-activation profiles were then inserted in the NRDL 704 computer program. By assuming a constant neutron field and a fixed percentage of manganese in the soil, the program computed the radiation field from each activation profile for all the stations and reactor heights for which data were obtained. A future NRDL report will discuss this program.³ Table 3.3 shows the resulting dose in roentgens per hour at 3 ft above the ground. The data taken at 30 yd show a reduction in the radiation field as the neutron source goes higher. A qualitative examination of color slides taken of the reactor at each height and from each station indicates that structure members of the tower are interposed between the reactor and the 30-yd station for reactor heights at 1125 and 1500 ft. The photographs also show that only the reactor at 1500 ft has attenuation present for the 100-yd station. The important point we should like to emphasize here is that we do not have enough data to make a precise calculation on the effect of the tower structure on the emitted neutron spectrum.

TABLE 3.3—CALCULATED ROENTGENS PER HOUR AT EACH STATION AND REACTOR HEIGHT FOR A GIVEN SULFUR FLUX AND AMOUNT OF MANGANESE IN THE SOIL AT EACH STATION

Reactor height, ft	Station					
	30 yd	100 yd	150 yd	200 yd	250 yd	300 yd
27	44.6*	33.6	33.6	34.7	31.0	33.7
299	42.1*	37.7	34.6	33.7	34.2	
500	39.7*		36.6			
1125	34.6†	34.3	34.7	34.7	33.5	34.9
1500	34.9†	28.9†		34.1		
Average = $34.3 \pm 3.8\%$						

*Neglected in the average because of excessive water content in the soil at time of data taking.

†Neglected in the average because of tower structure effects on the neutron spectrum.

The computed radiation fields at the reactor heights of 500, 299, and 27 ft for the 30-yd station were greater than the average radiation-field value at the other stations because the data for the 30-yd station were taken early in April whereas data for the other stations were taken in late May and in June. During this time there was a dramatic change in moisture content of the soil, and the effect can be seen in Figs. 3.7 and 3.8. The change in moisture content of the soil changes the activation profile in the soil and the resultant radiation field.

Because of the interference and uncertainty resulting from structure effects of the tower and moisture content of the soil, we ignored these marked stations and looked at effects of height and distance from the tower on the other stations. The average dose rate over the rest of the stations is $34.3 \text{ r/hr} \pm 10\%$, and there is no apparent systematic effect caused by the height and the distance from the source.

Figure 3.3E shows the thermal-neutron flux averaged over all stations for each reactor height. There is definitely a changing profile with reactor height, but in the first 6 in. of the soil there is very little variation. The computer program indicates that 77% of the observed radiation comes from the first 6 in. of soil, and this is one of the factors that limits any change in the radiation field when there are small changes in the activation profile in the ground.

Measurements were made on the activation of ^{55}Mn , both with and without cadmium covers on the samples. With the use of our data for the activation of manganese by neutrons with energies above the cadmium cutoff energy, which were normalized at the surface in Fig. 3.11, the same computer program and conditions were used to determine what percentage of the total radiation field came from activated manganese by other than thermal neutrons. Table 3.4 shows the percentage of the total dose that is contributed by manganese activated by neutrons with energies above the cadmium cutoff energy, which averages to 13% of the dose that is due to the spectrum of all neutron energies.

TABLE 3.4 — PERCENTAGE OF THE TOTAL RADIATION FIELD THAT IS CONTRIBUTED BY MANGANESE ACTIVATED BY NEUTRONS ABOVE THE CADMIUM CUTOFF ENERGY

Height of reactor, ft	Station, yd	Percentage
1125	200	12.2
500	150	12.8
299	150	15.5
27	150	13.2
500	30	9.7
Average = $12.7 \pm 2.7\%$		

An evaluation of the effect of controlled moisture was attempted by adding moisture to the soil at one station. The difficulty of adding moisture to a large area, especially in the desert, can be shown by our effort to increase the moisture content around one station. Two thousand gallons of water were dumped into a 12-ft-diameter circle that was ditched to help confine the water. The water was delivered in the night, and the next day a sample was taken to see how much moisture had been retained. The following table describes the conditions:

Soil depth	Before	After
0 to 3 in.	1.0% H_2O	5.2% H_2O
3 to 6 in.	3.9% H_2O	7.0% H_2O

The difficulty of getting water to the area and the rapid evaporation lead one to feel that it would take at least 10,000 gal to saturate this soil with moisture.

3.2 SUMMARY

When tactical nuclear weapons are used so as to minimize local fallout, the most important residual hazard is neutron-induced radioactivity in the soil. The "no fallout" condition is obtained by detonating the weapon so that the fireball does not touch the ground. Therefore study of the neutron-induced soil activity due to a neutron source in the air was important; this was the objective of Program 5.

Operation BREN was an experiment that used a 1500-ft tower and an unshielded fast reactor similar to "Godiva" to simulate the neutron flux from a nuclear detonation.

Samples of manganese, cadmium-covered manganese, gold, cadmium-covered gold, and sulfur were placed from 0 to 20 in. in the ground and at distances out to 400 yd from the base of the tower. The reactor was then operated at various heights so that the effect of the height of a neutron source on the neutron-induced activity of a soil could be studied.

No systematic effect due to the variation in soil composition or to the effect of reactor height was present which would change the manganese activation profiles sufficiently to cause a corresponding change in the computed radiation field of greater than $\pm 10\%$. Manganese activated by epithermal neutrons contributed 13% of the total radiation field.

3.3 CONCLUSIONS

Through the BREN experiment three important effects of induced activity from a nuclear detonation were determined, the effect of the height of the weapon, the effect of distance from Ground Zero, and the effect of activation of manganese by neutrons with energy greater than that of thermal neutrons. By normalizing each manganese activation profile for every reactor height and station and then using these profiles in our computer program, we were able to compute the dose rate due to radiation field at every station. Examination of the results shows the greatest deviation of dose rate from the average to be 11%, and no systematic error was noted. The activation of manganese by neutrons with energies above the thermal region could make a contribution in the manganese radiation field of 13% of the total dose rate for this source.

REFERENCES

1. R. L. Mather, *Neutron Distributions near an Air-Soil Boundary as a Function of Soil-water Content*, Report USNRDL-TR-465, Naval Radiological Defense Laboratory, Sept. 28, 1960. (Classified)
2. F. M. Tomnovec and R. L. Mather, *The Influence of Soil Composition on the Thermal Neutron Component of Large Scale Neutron Fields*, Report USNRDL-TR-413, Naval Radiological Defense Laboratory, July 19, 1960.
3. P. A. Read, *Calculations and Nomograms for a Neutron-induced Activity Prediction System*, to be published at Naval Radiological Defense Laboratory.

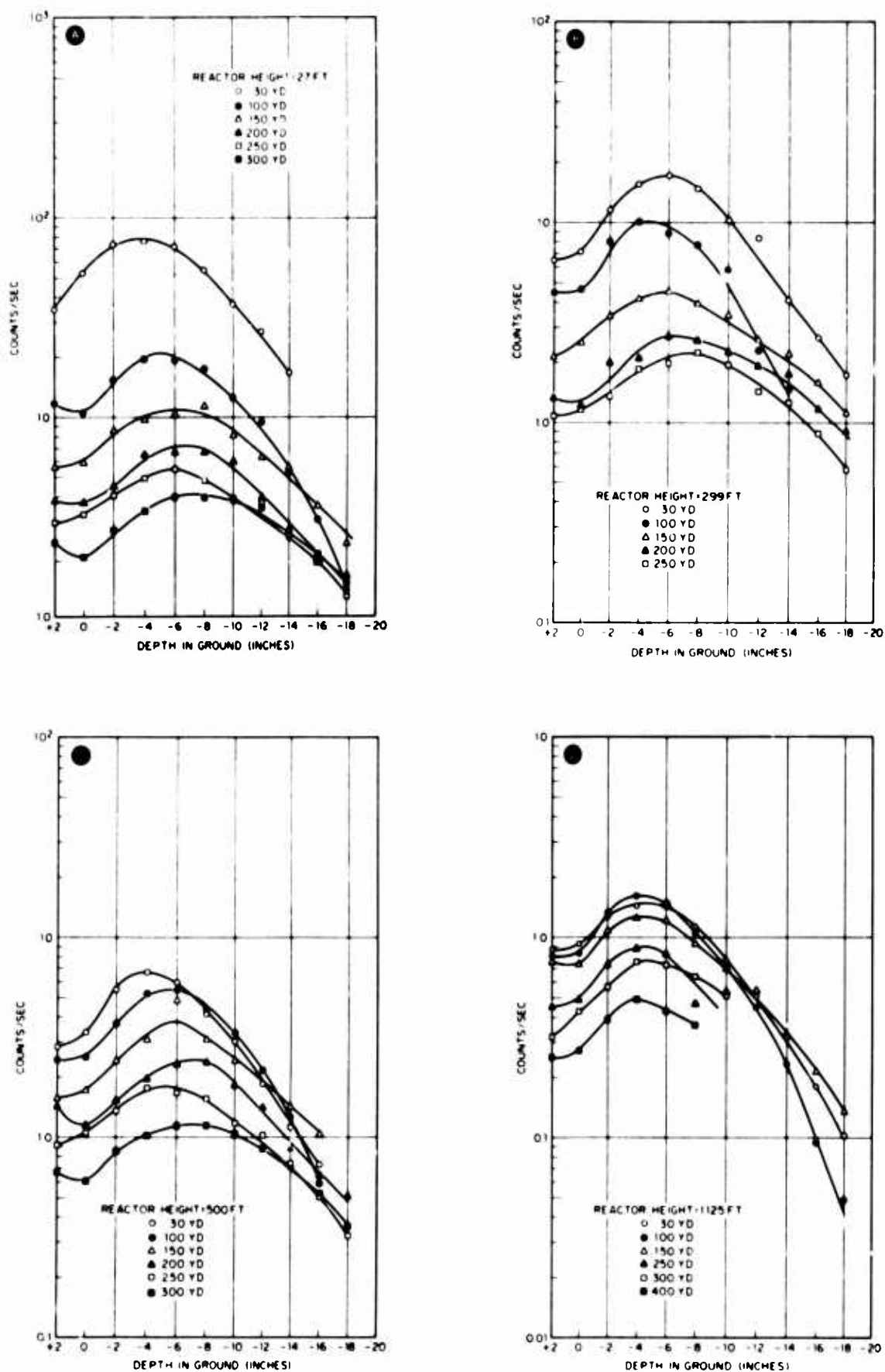


Fig. 3.1—Relative gold thermal-neutron activation as a function of depth. These data were obtained by subtracting the specific activity in a cadmium-covered gold sample from that in a bare gold sample at the same position. Parts A, B, C, and D are for reactor heights of 27, 299, 500, and 1125 ft, respectively.

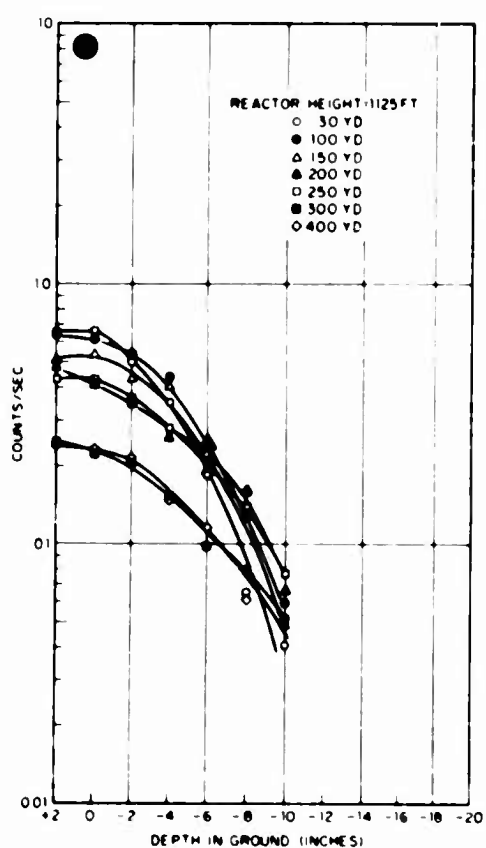
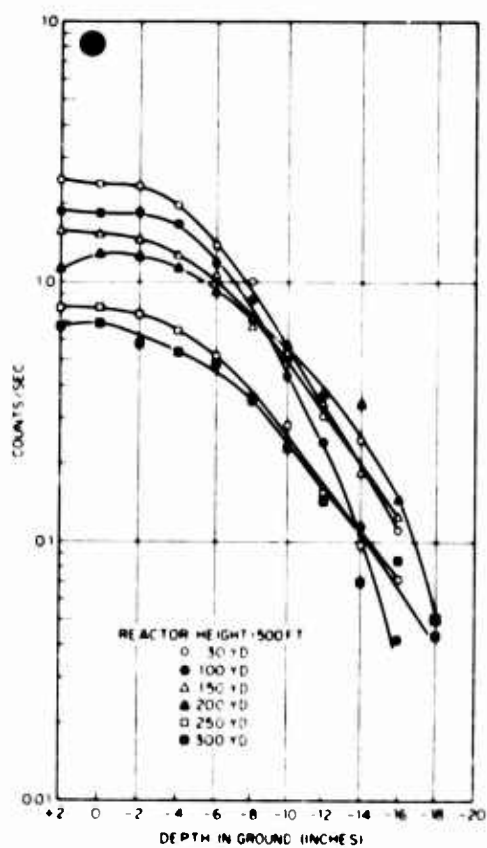
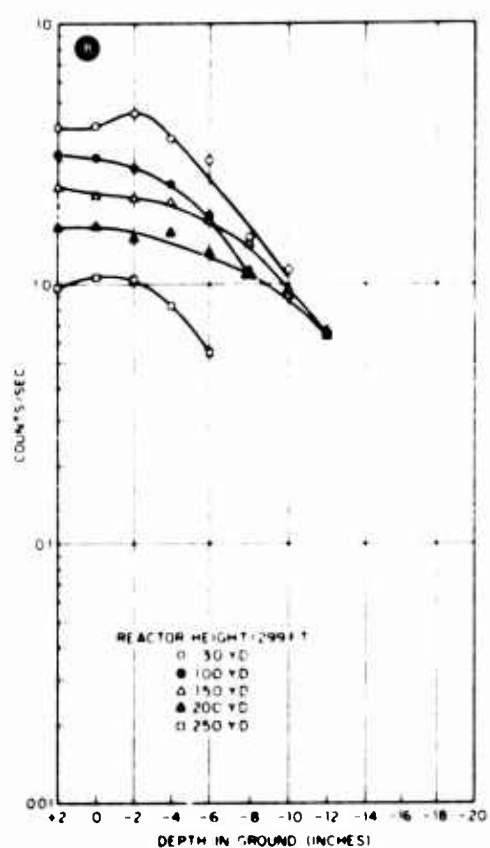
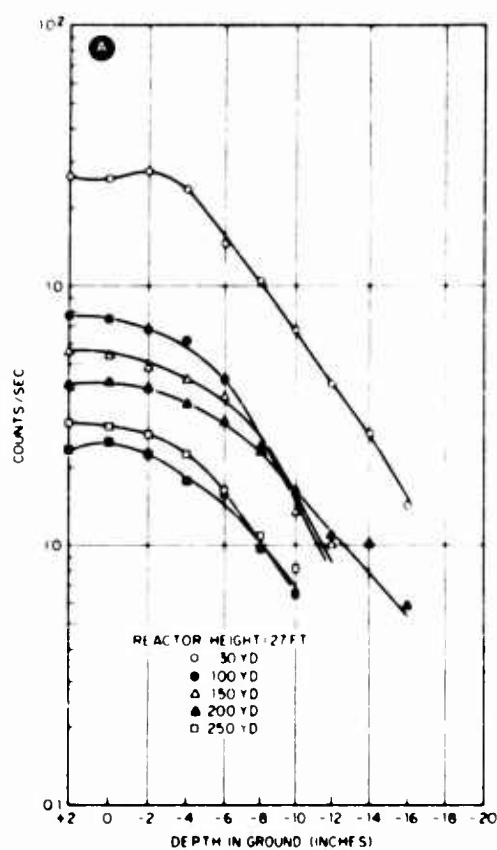


Fig. 3.2—Gold epithermal activations vs. depth. These data represent the activity in cadmium-covered gold samples. Parts A, B, C, and D are for reactor heights of 27, 299, 500, and 1125 ft, respectively.

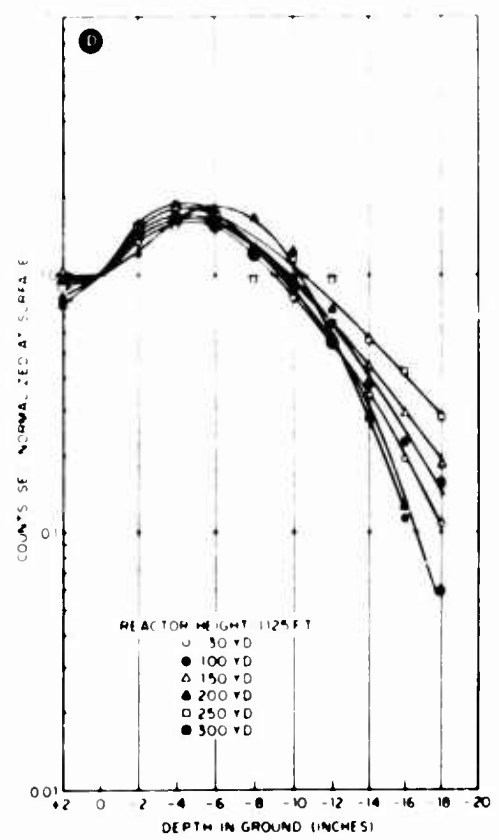
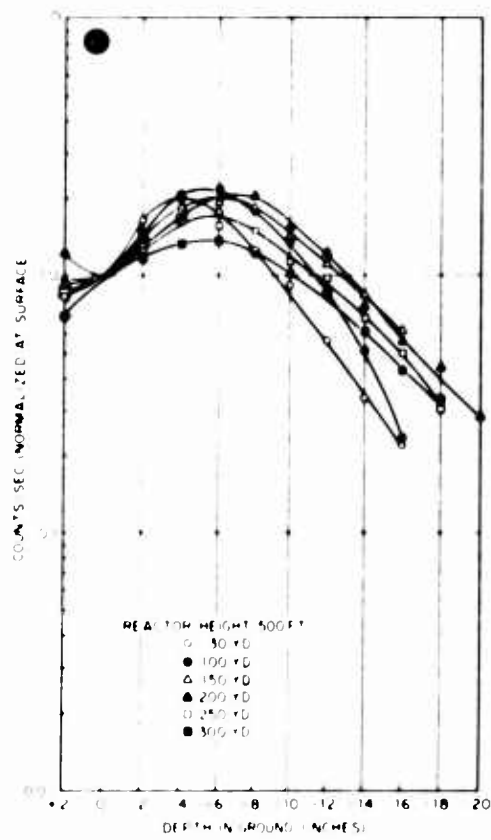
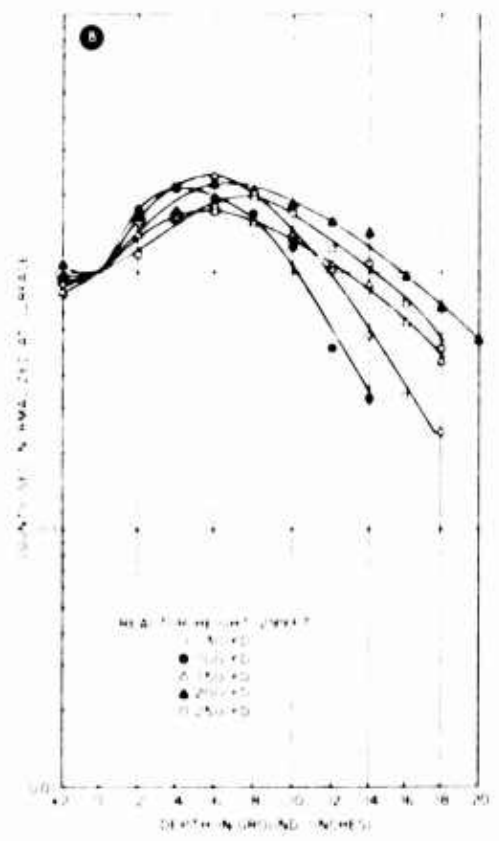
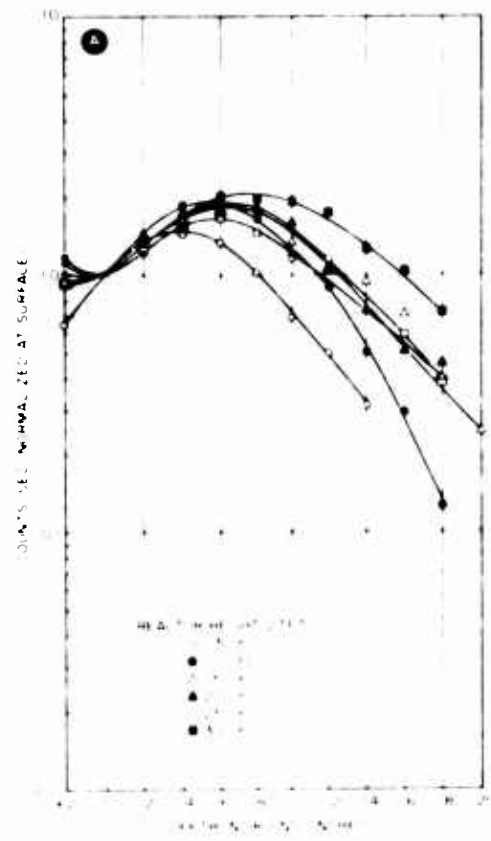


Fig. 3.3—(See following page for legend.)

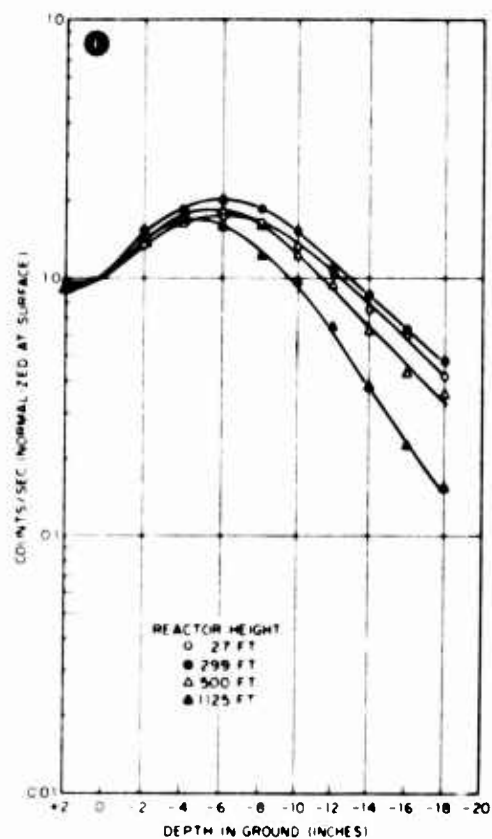


Fig. 3.3—Gold thermal activation vs. depth, normalized at the surface. These are the same data as in Fig. 3.1 except that the curves for the different stations were normalized at the surface in order to compare the shapes of the curves. Figure 3.3E is the one curve for all stations at each reactor height.

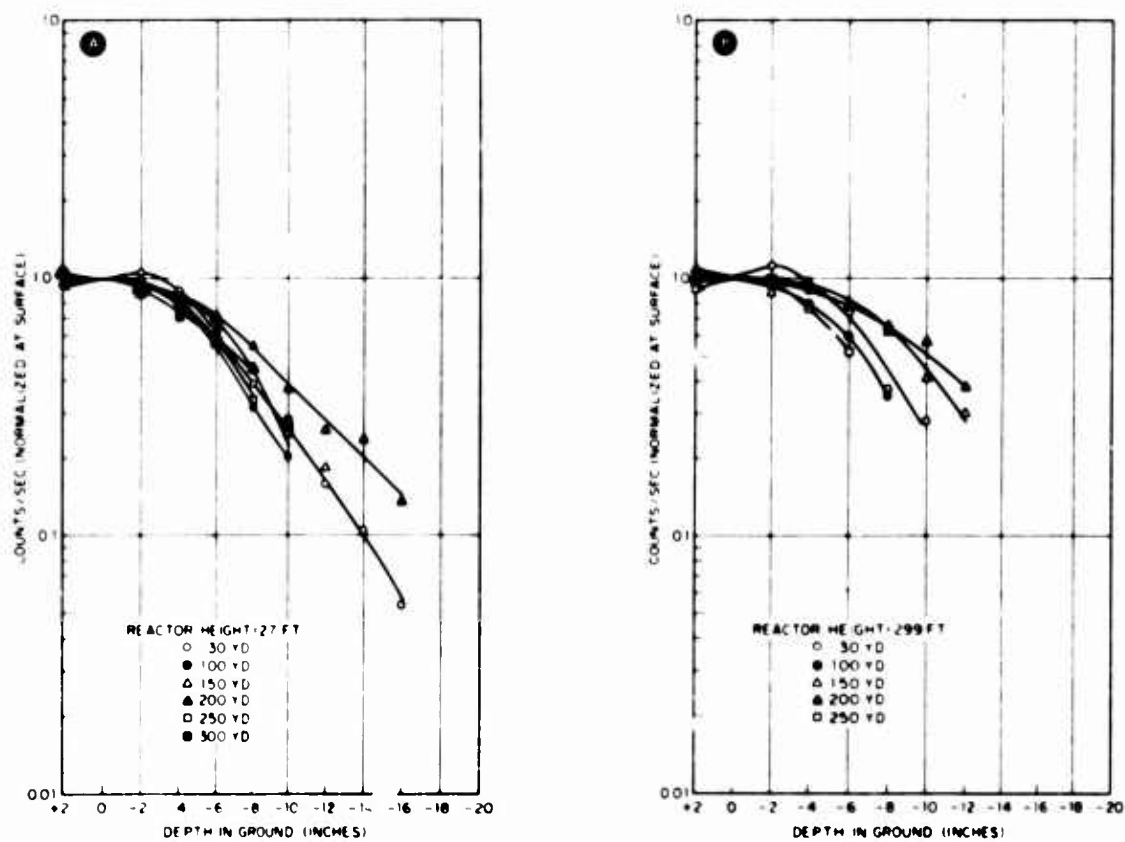


Fig. 3.4—(See following page for legend.)

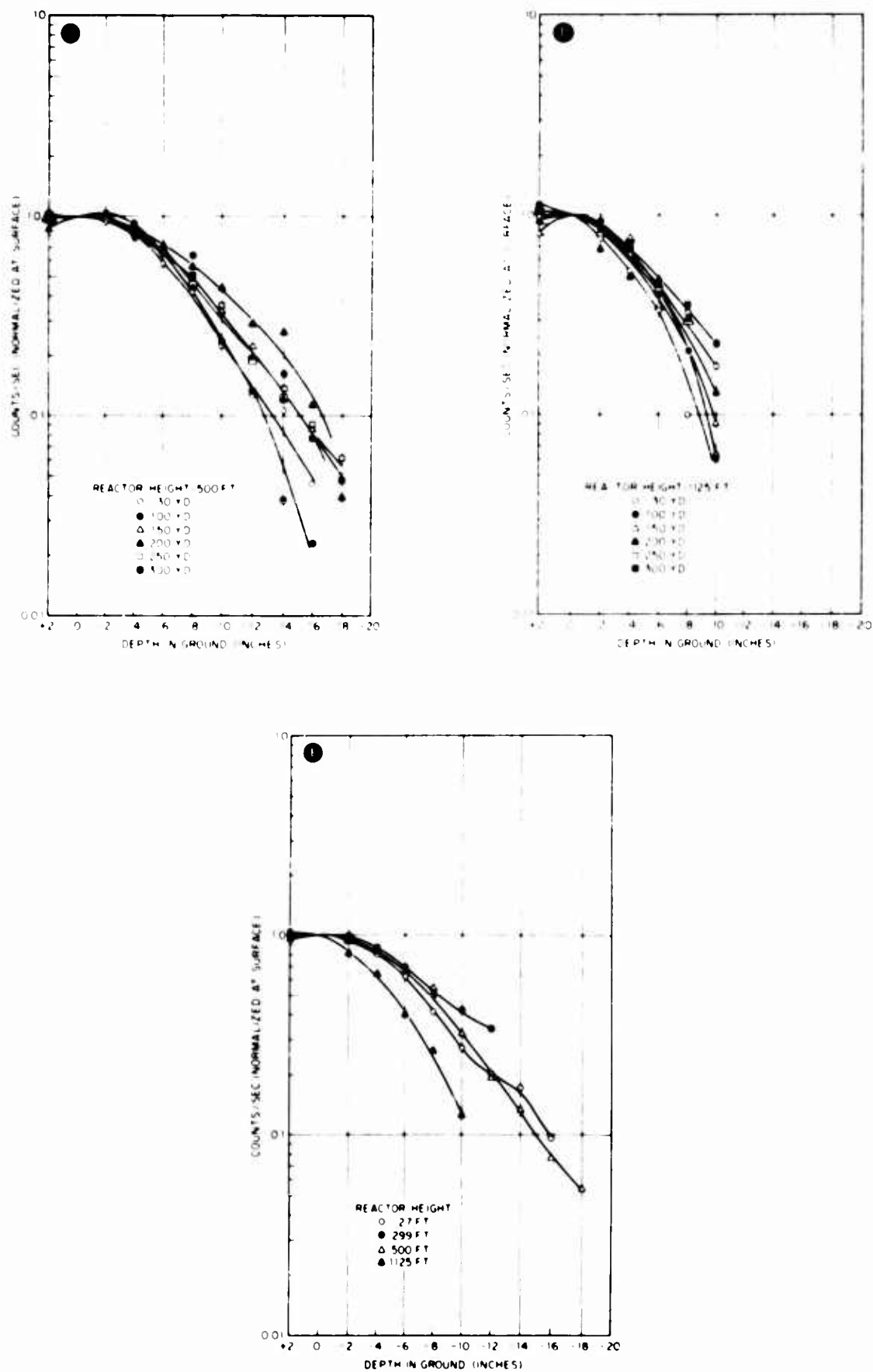


Fig. 3.4—Gold epithermal activation vs. depth, normalized at the surface. These are the same data as in Fig. 3.2 except that curves for the different stations were normalized at the surface in order to compare the shapes of the curves. Figure 3.4 is the average of all stations for each reactor height.

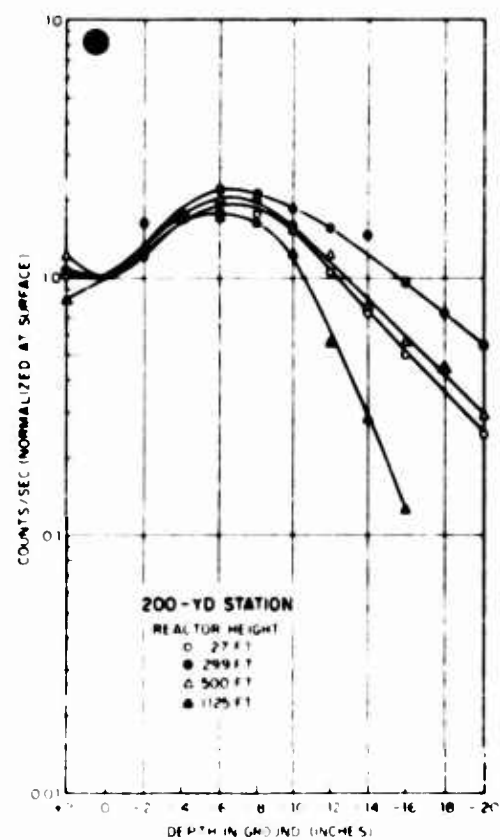
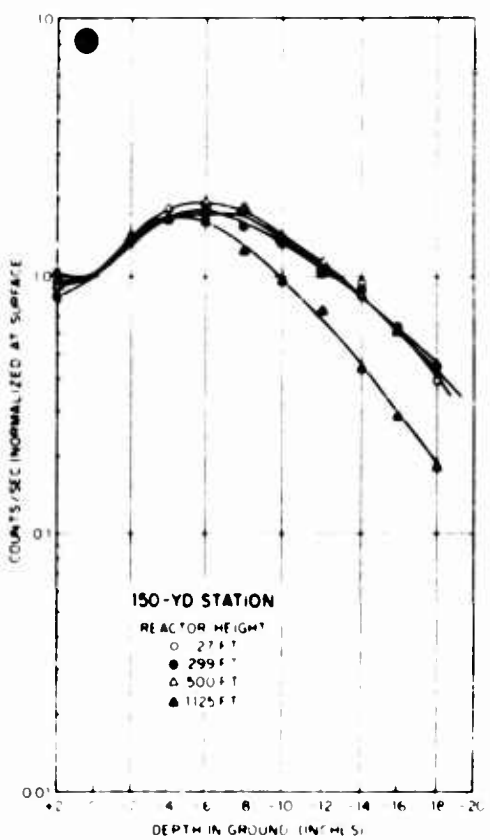
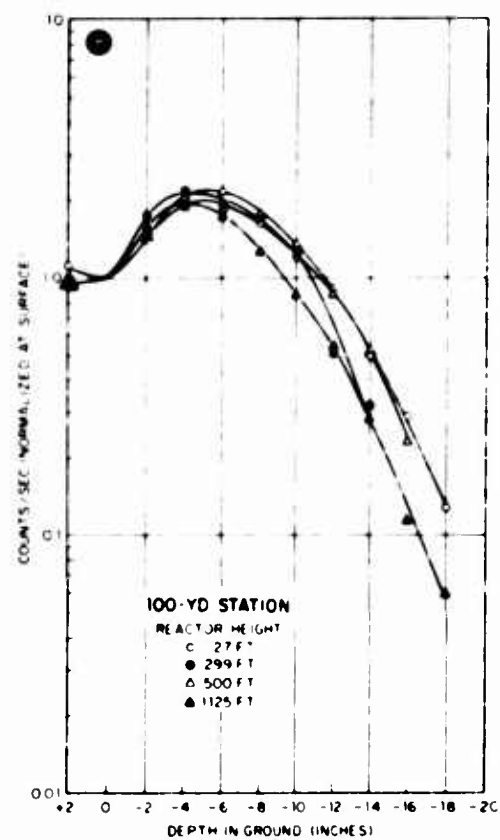
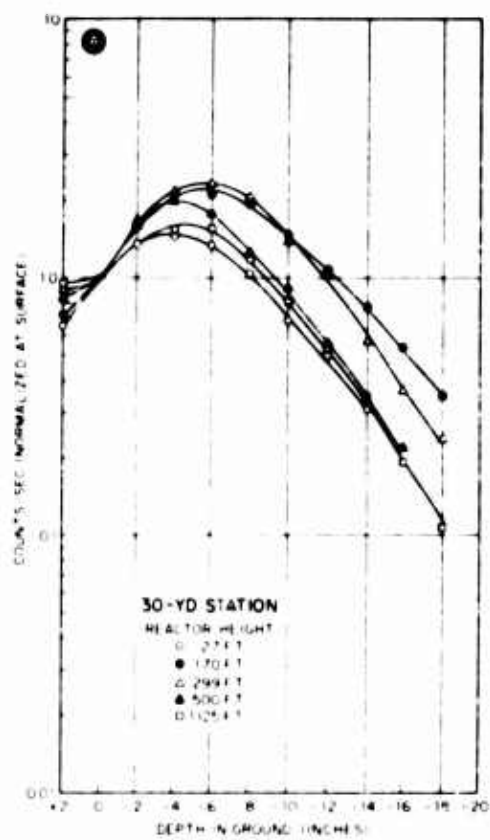


Fig. 3.5—(See following page for legend.)

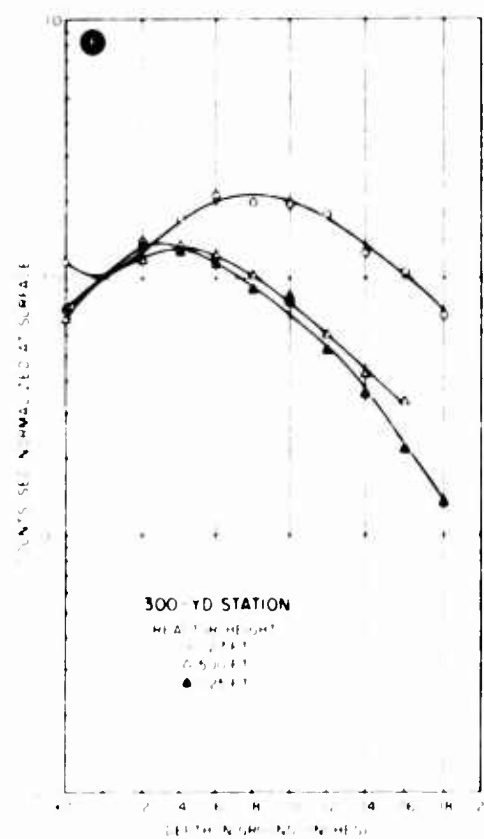
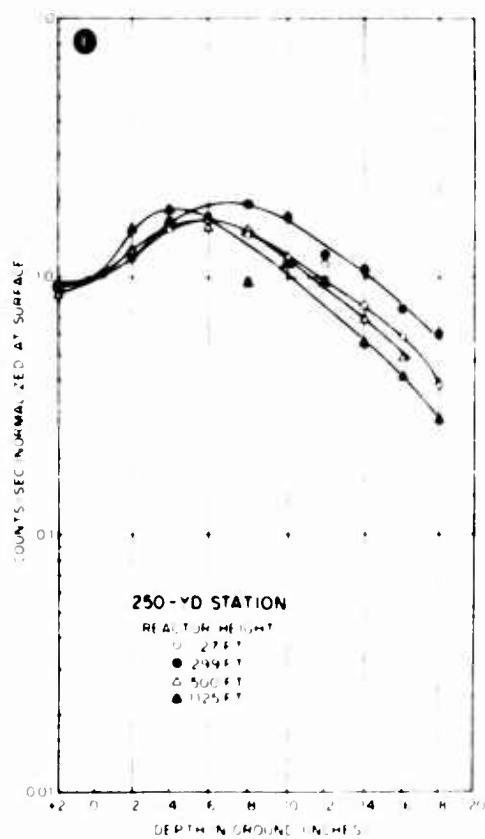


Fig. 3.5—Gold thermal activation vs. depth, normalized at the surface. This is a replot of the data in Fig. 3.3, but, instead of comparing different stations for the same reactor height, each station is plotted separately, with varying reactor heights. Parts A, B, C, D, E, and F refer to 30-, 100-, 150-, 200-, 250-, and 300-yd stations, respectively.

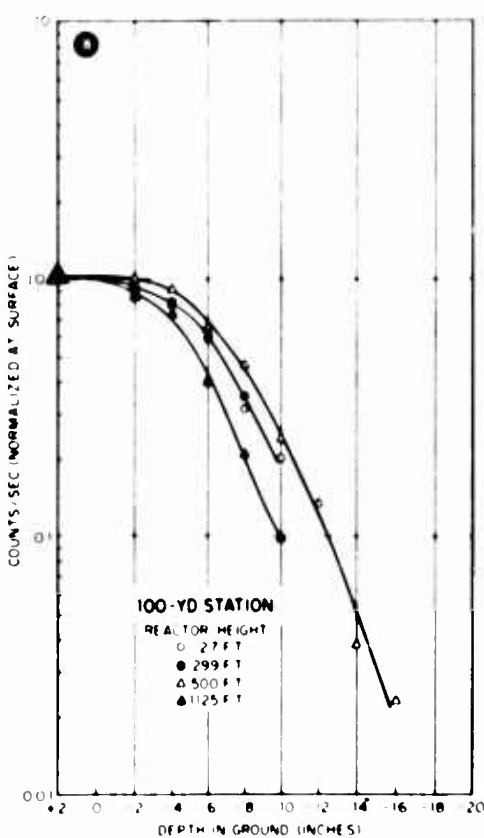
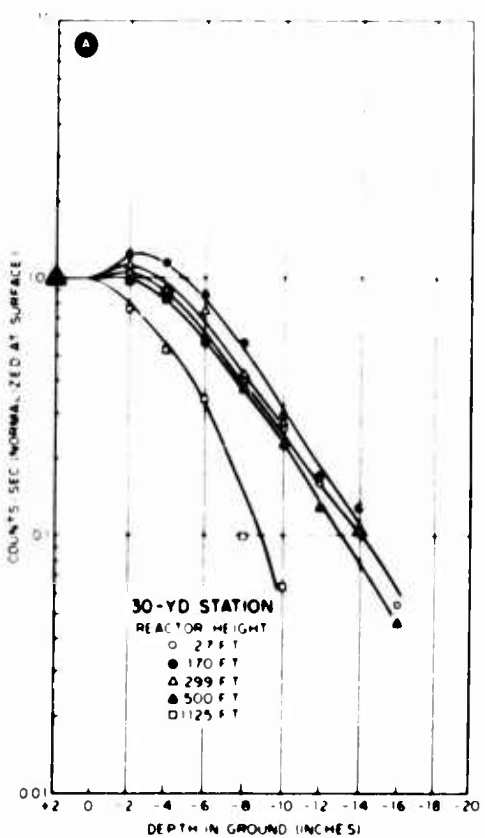


Fig. 3.6—(See following page for legend.)

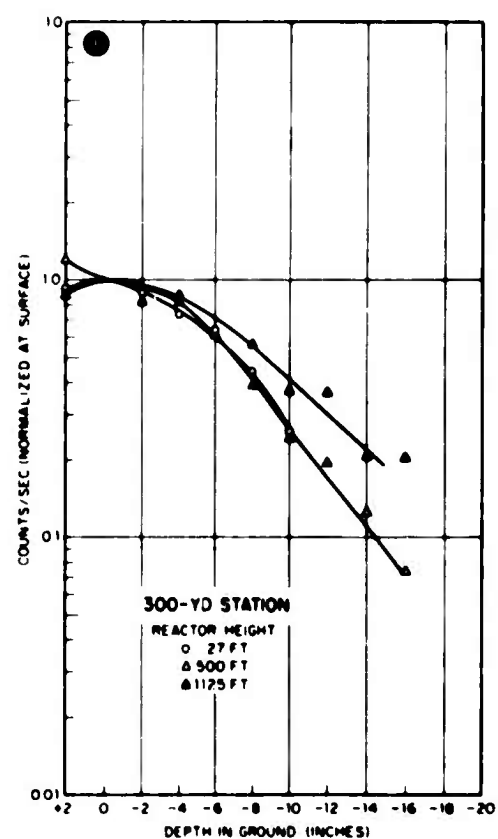
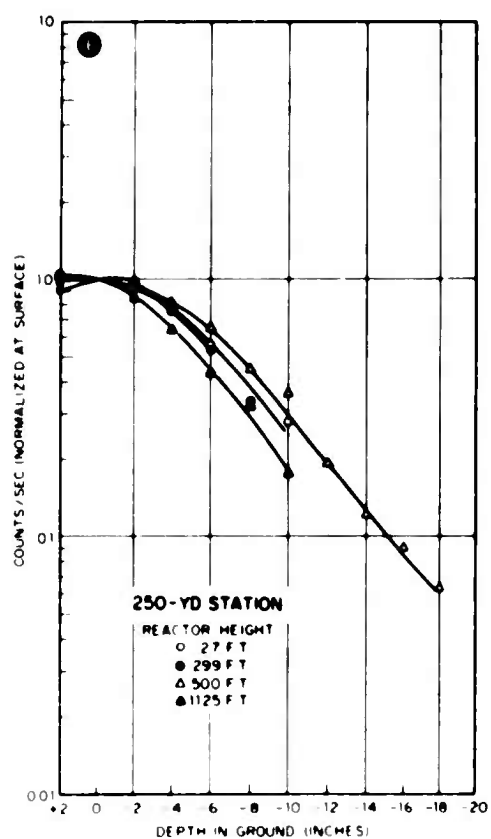
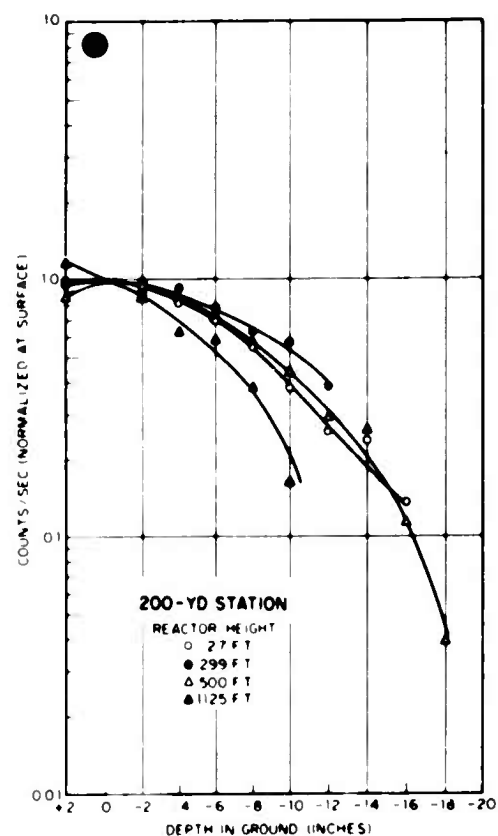
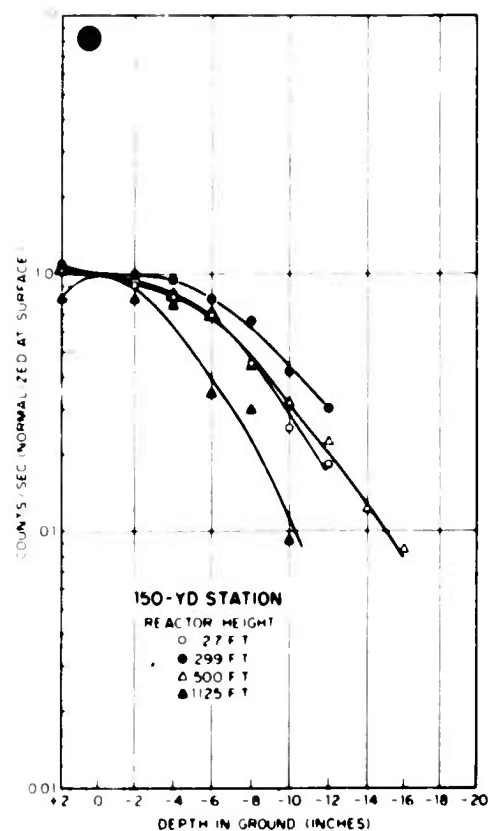


Fig. 3.6—Gold epithermal activation vs. depth, normalized at the surface. This is a replot of the data in Figs. 3.2 and 3.4, but, instead of comparing different stations for the same reactor height, each station is plotted separately, with varying reactor heights. Parts A, B, C, D, E, and F refer to 30-, 100-, 150-, 200-, 250-, and 300-yd stations, respectively.

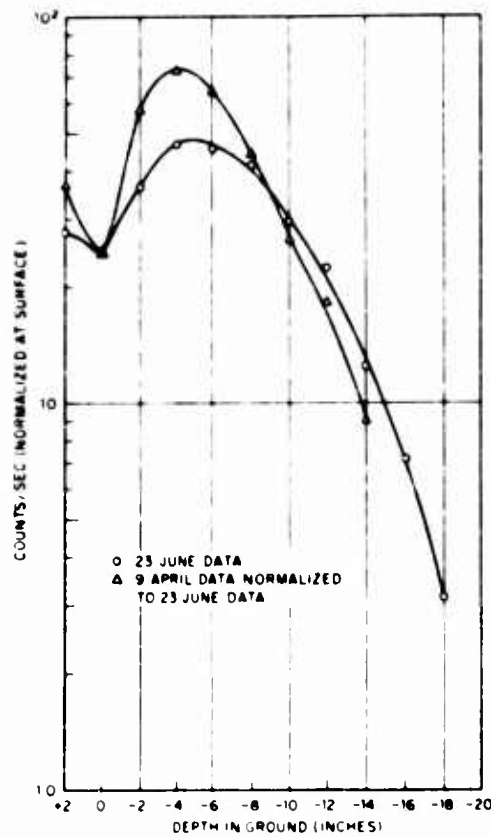


Fig. 3.7—Gold thermal activation vs. depth for the 100-yd station and 27-ft reactor height. The two sets of data were taken under identical conditions except that during the period between runs the soil had dried out, changing its moderating properties. See Table 3.2 and Fig. 3.8 for rainfall and moisture in this time period.

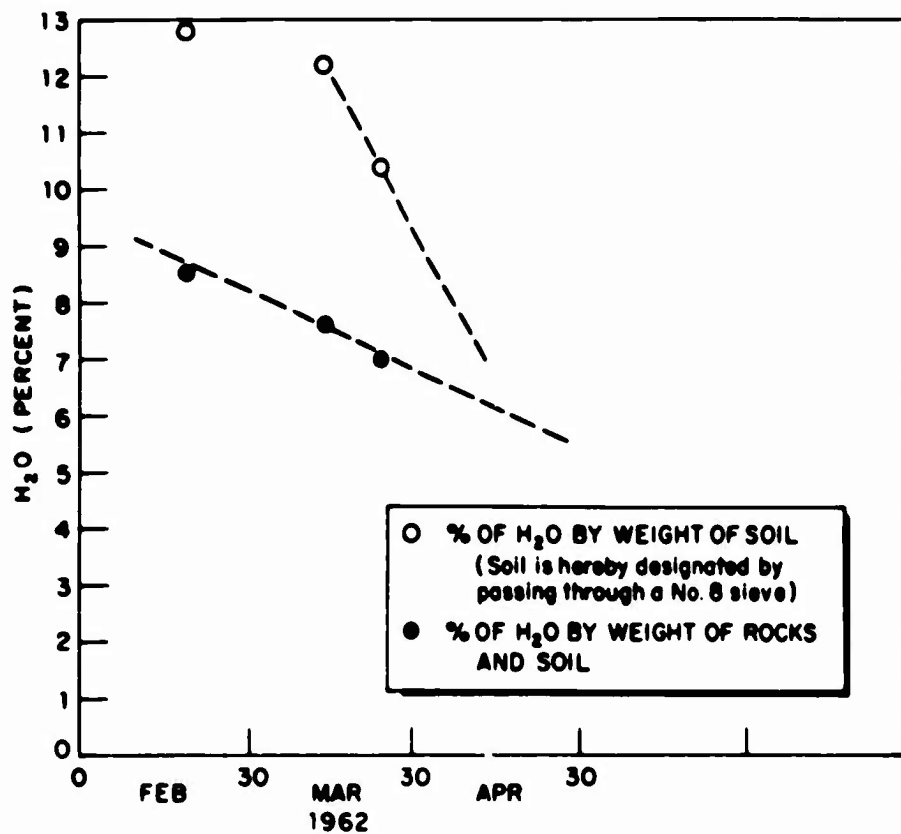


Fig. 3.8—Soil moisture content vs. time. This curve shows how the soil moisture content varied during the course of the experiment. The data represent averages over all the stations.

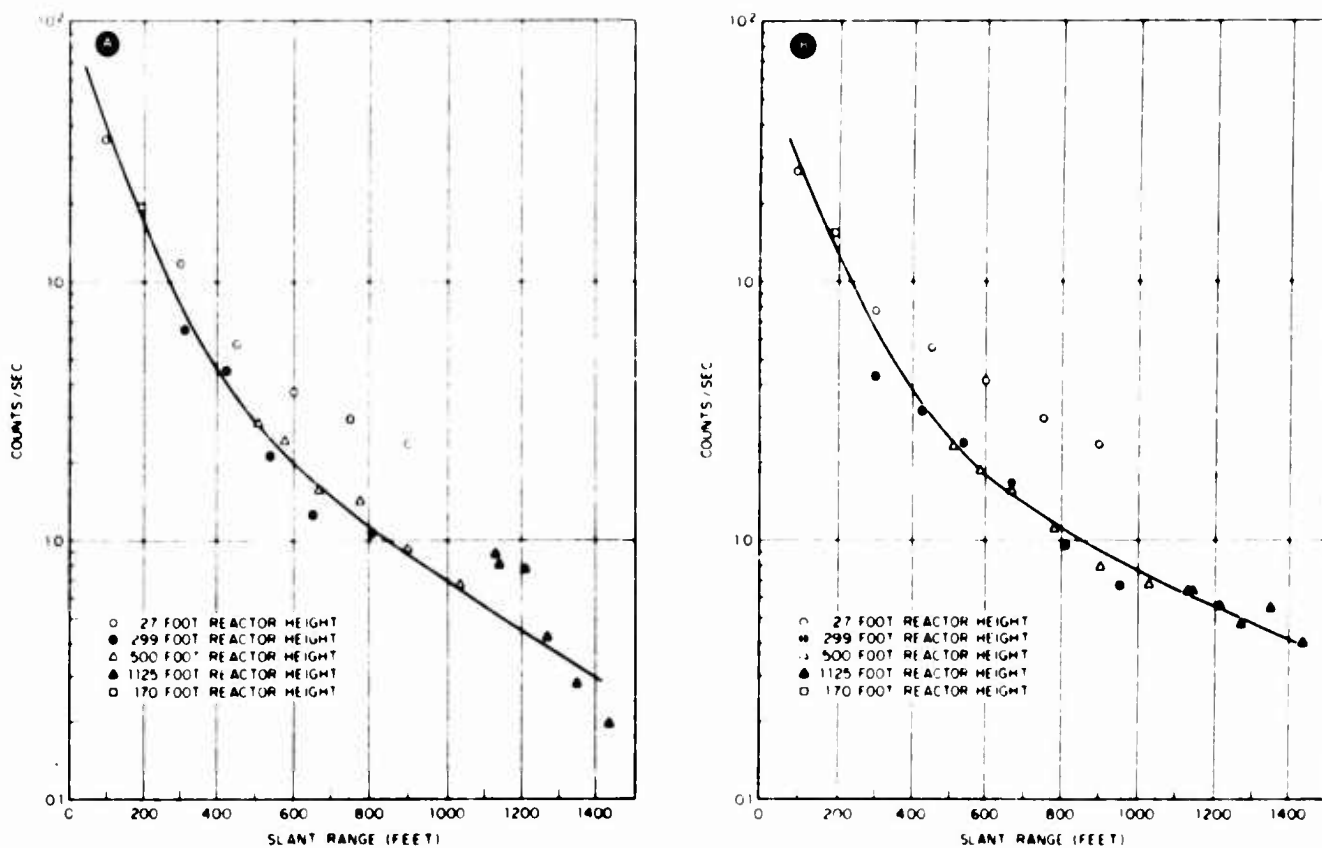


Fig. 3.9—Surface gold activation vs. slant range. Part A gives the relative activation produced by neutrons below the cadmium cutoff, obtained by subtracting the specific activity of a cadmium-covered gold sample from that of a bare gold sample at the same location. Part B gives the relative activation of gold produced by neutrons above the cadmium cutoff, obtained from the specific activities of cadmium-covered gold samples. Data for different reactor heights are marked by different kinds of points. Runs were normalized to each other. The solid line indicates the major trend of the points.

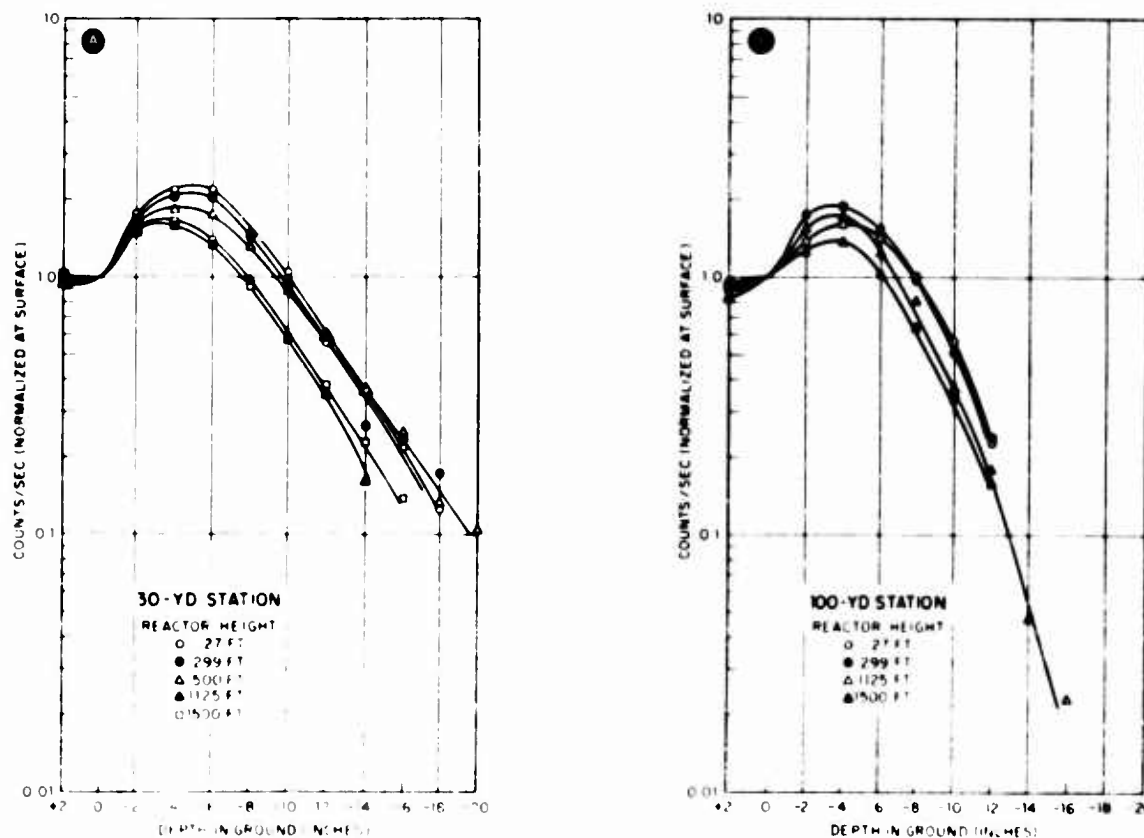


Fig. 3.10—(See following page for legend.)

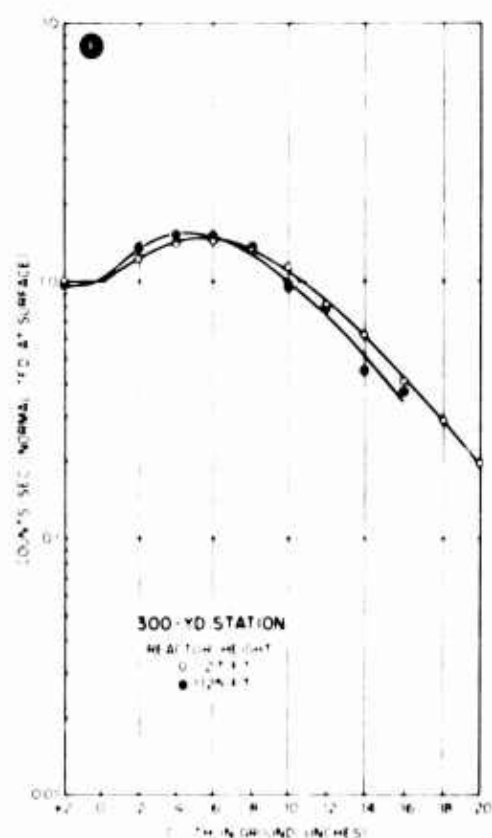
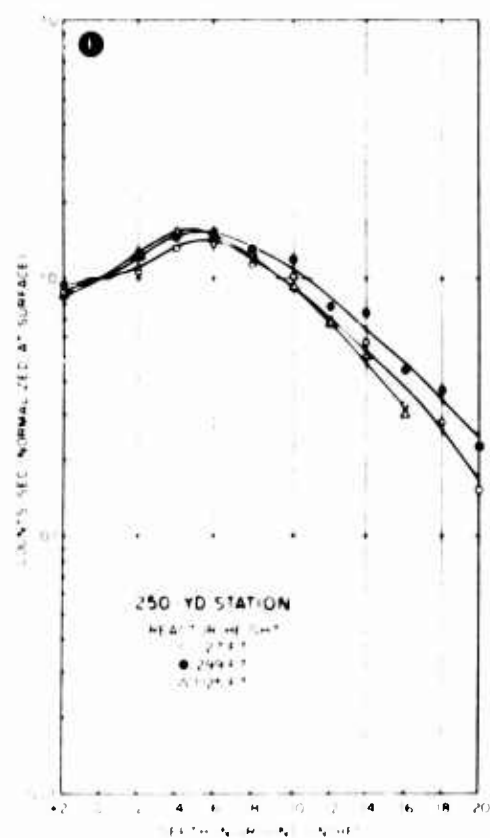
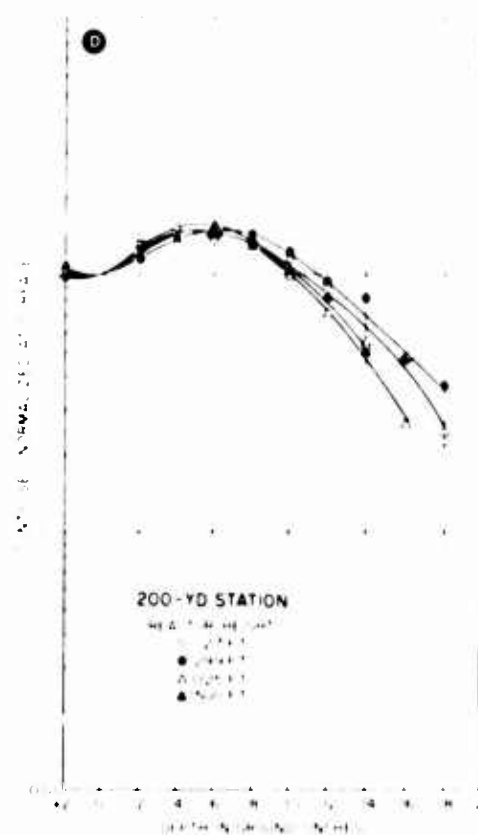
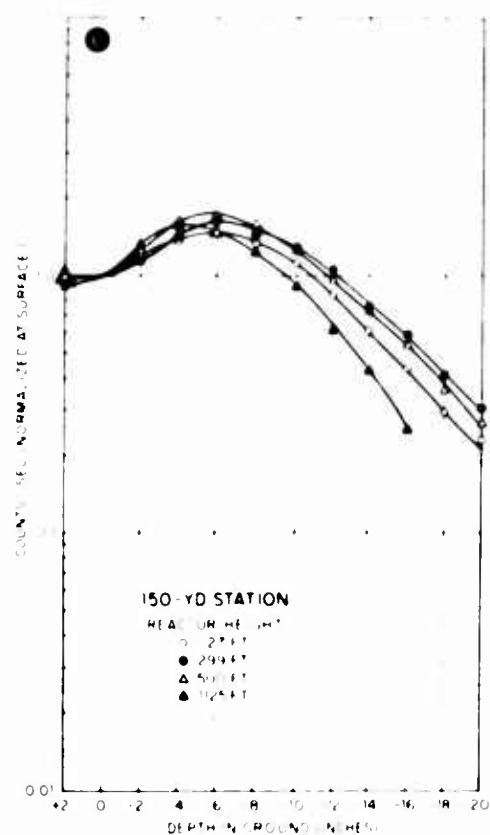


Fig. 3.10—Manganese activation vs. depth. These data represent the relative activities of bare manganese samples. For each station the data have been normalized at the surface to compare the shapes of the curves. Parts A, B, C, D, E, and F are data for the 30-, 100-, 150-, 200-, 250- and 300-yd stations, respectively.

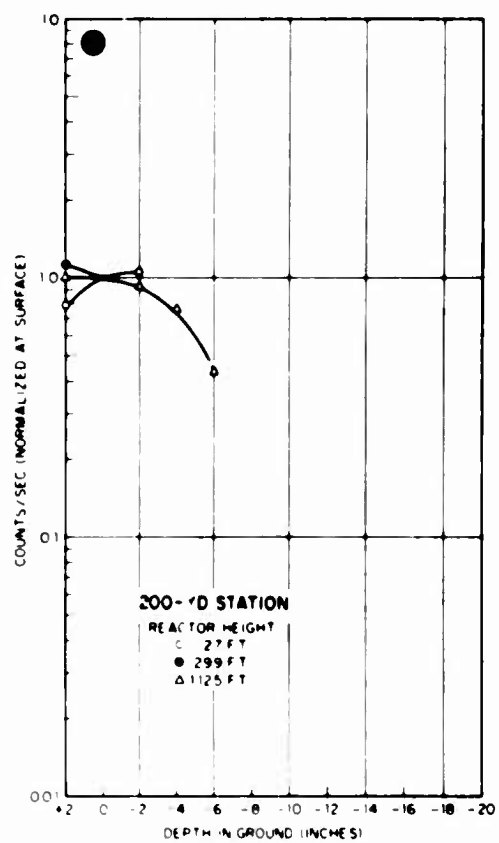
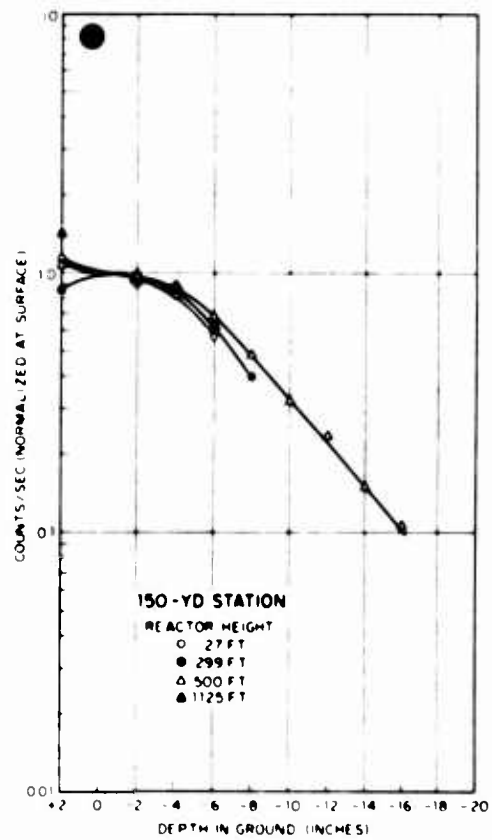
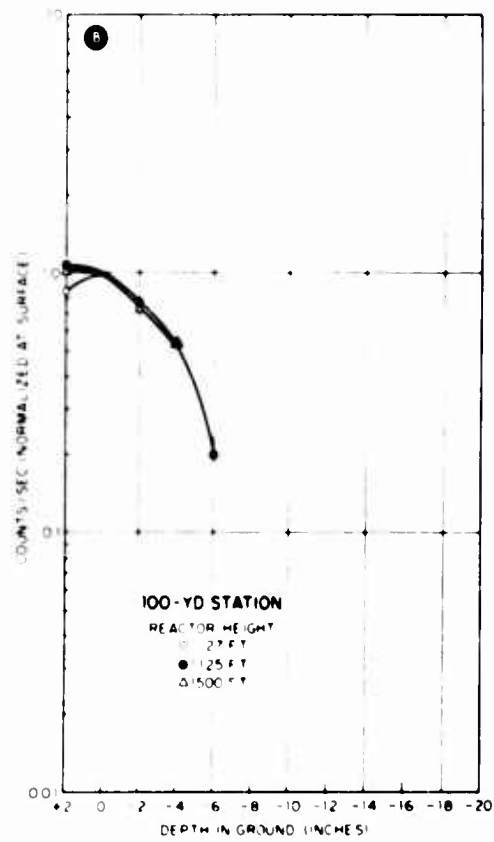
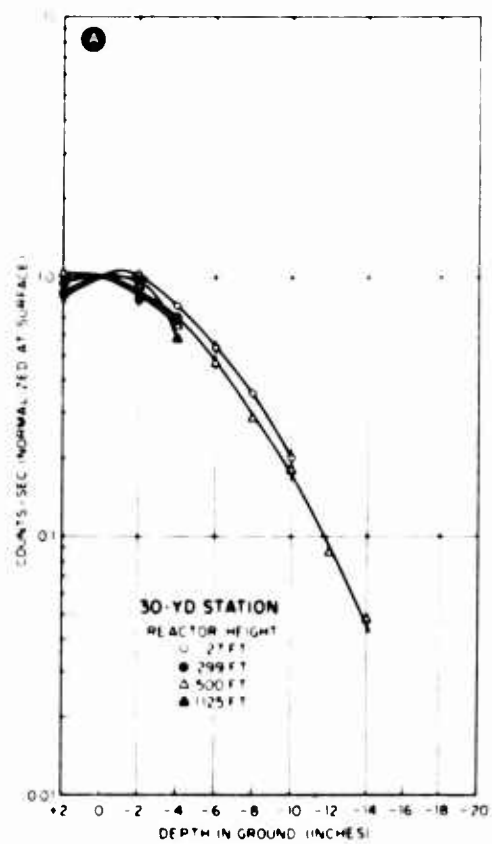


Fig. 3.11—(See following page for legend.)

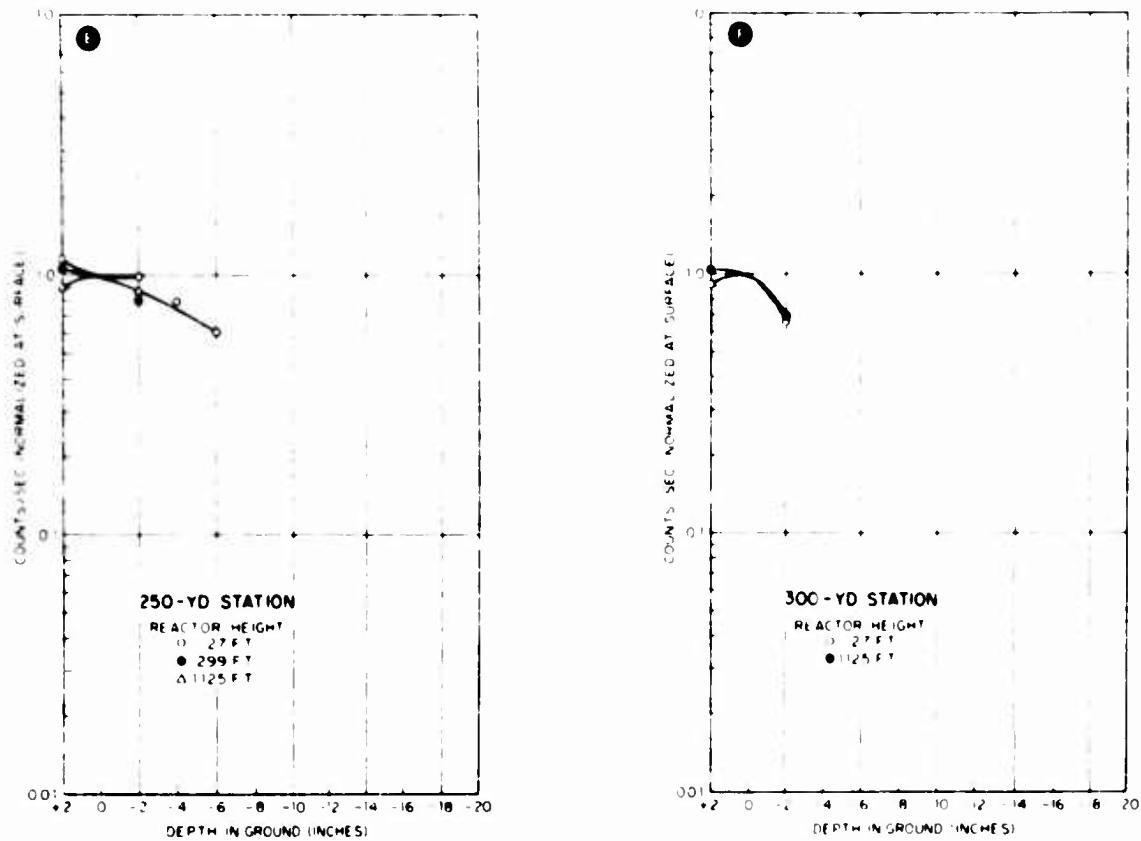


Fig. 3.11—Manganese epithermal activation vs. depth. These data represent the relative activities of cadmium-covered manganese samples. For each station the data have been normalized at the surface to compare the shapes of the curves. Parts A, B, C, D, E, and F are data for the 30-, 100-, 150-, 200-, 250-, and 300-yd stations, respectively. Lines are drawn through the points corresponding to the same height in slant range to guide the eye, although in some cases there are not enough data to define clearly the trend of the curve.

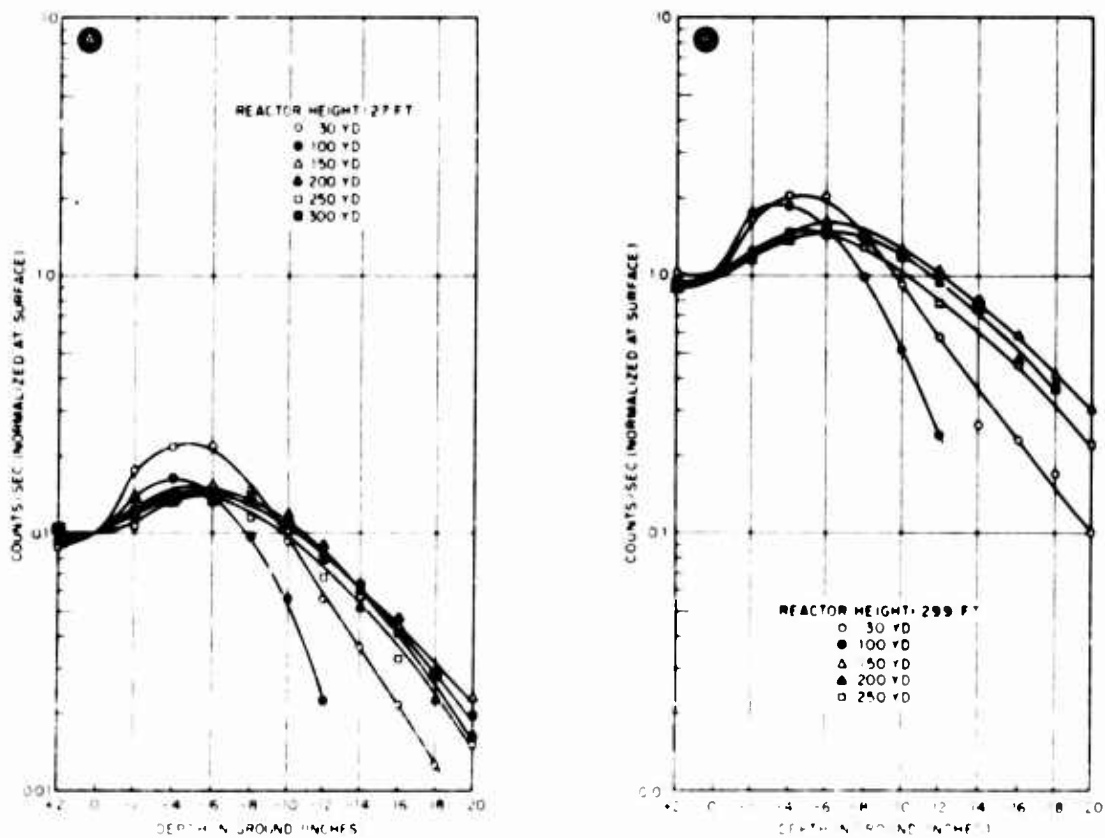


Fig. 3.12—(See following page for legend.)

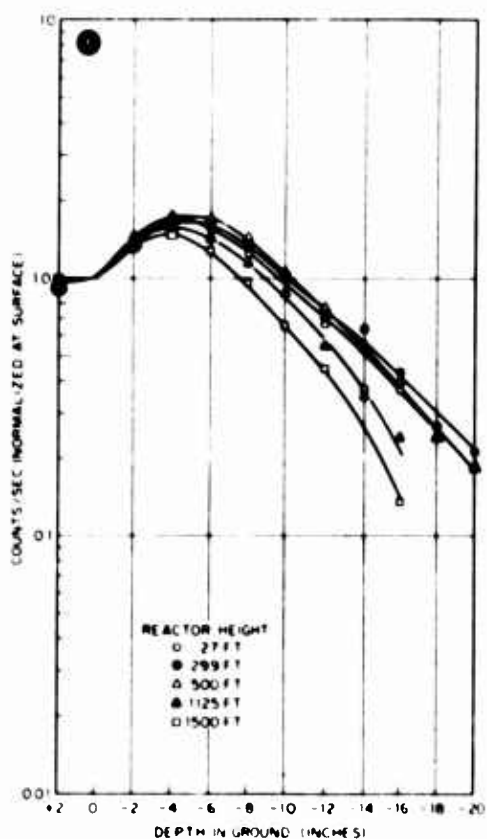
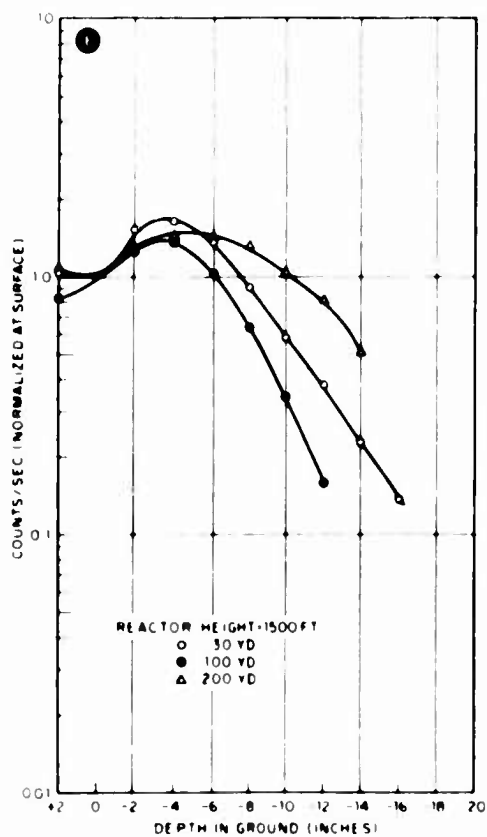
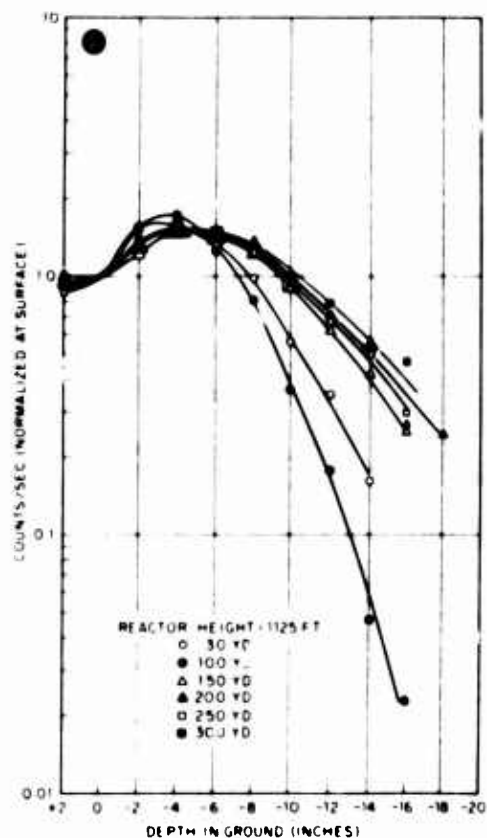
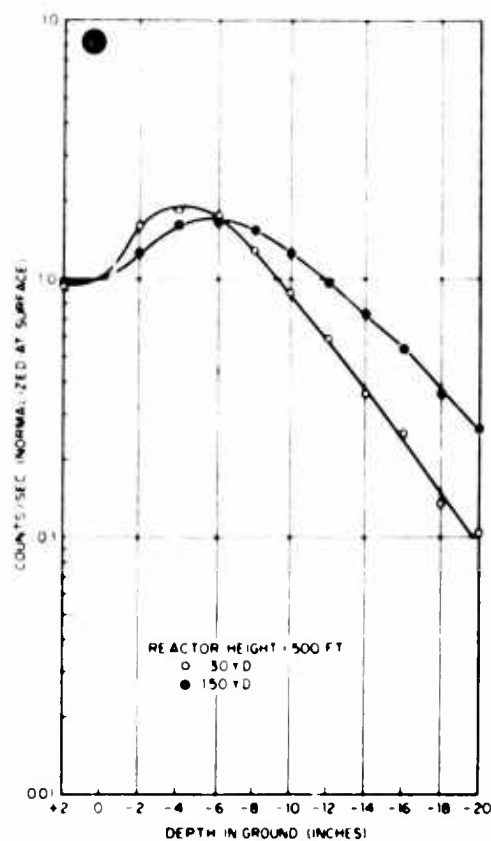


Fig. 3.12—Manganese activation vs. depth. These are the same data as in Fig. 3.10, but, instead of comparing different reactor heights for the same station, each reactor height is compared separately, with varying stations. Parts A, B, C, D, and E are for reactor heights of 27, 299, 500, 1125, and 1500 ft, respectively. Part F gives curves averaged over all stations for each reactor height.

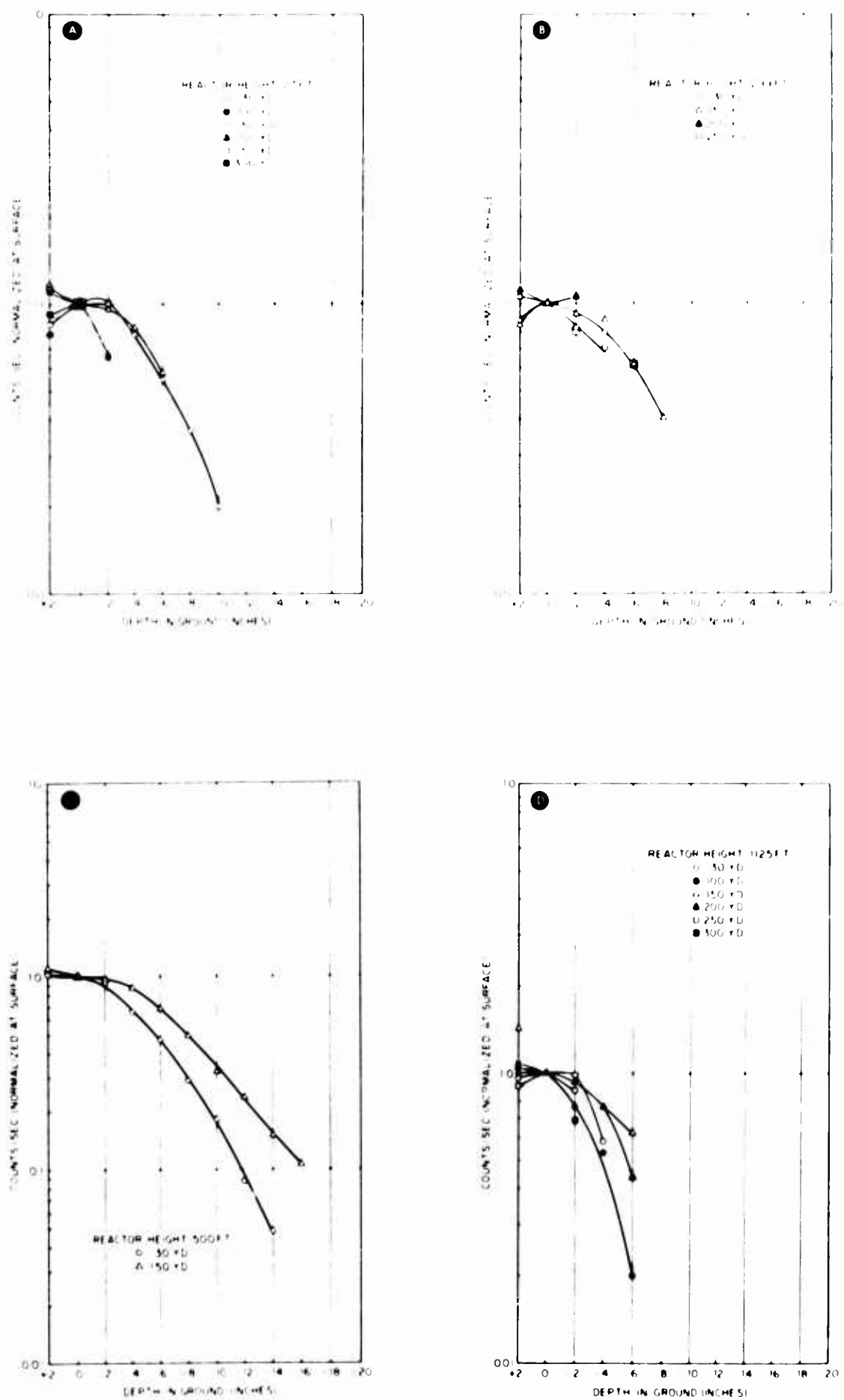


Fig. 3.13—(See following page for legend.)

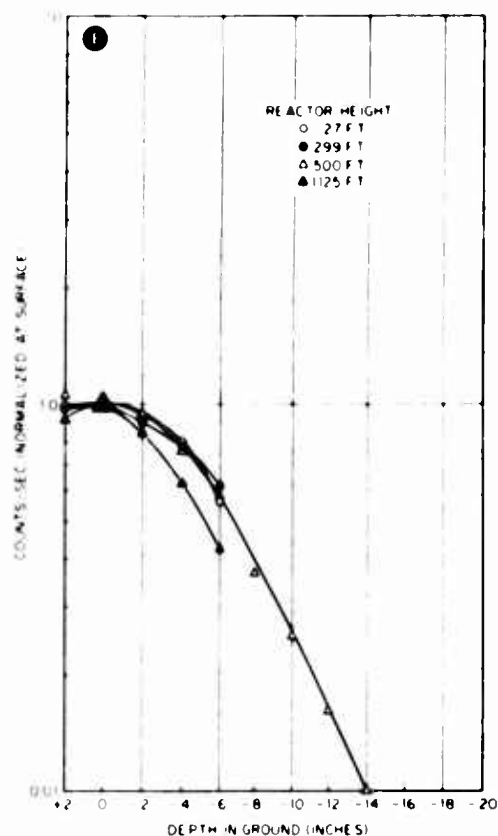


Fig. 3.13—Manganese epithermal activation vs. depth. These are the same data as in Fig. 3.11, but, instead of different reactor heights for the same station being compared, each reactor height is compared separately, with varying stations. Parts A, B, C, and D are for reactor heights of 27, 299, 500, and 1125 ft, respectively. Part E gives curves averaged over all stations for each reactor height.

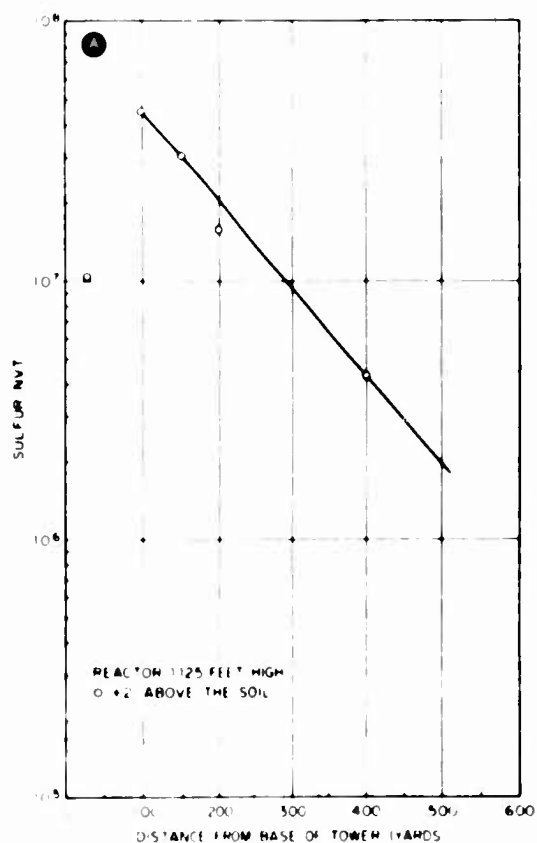


Fig. 3.14—(See following page for legend.)

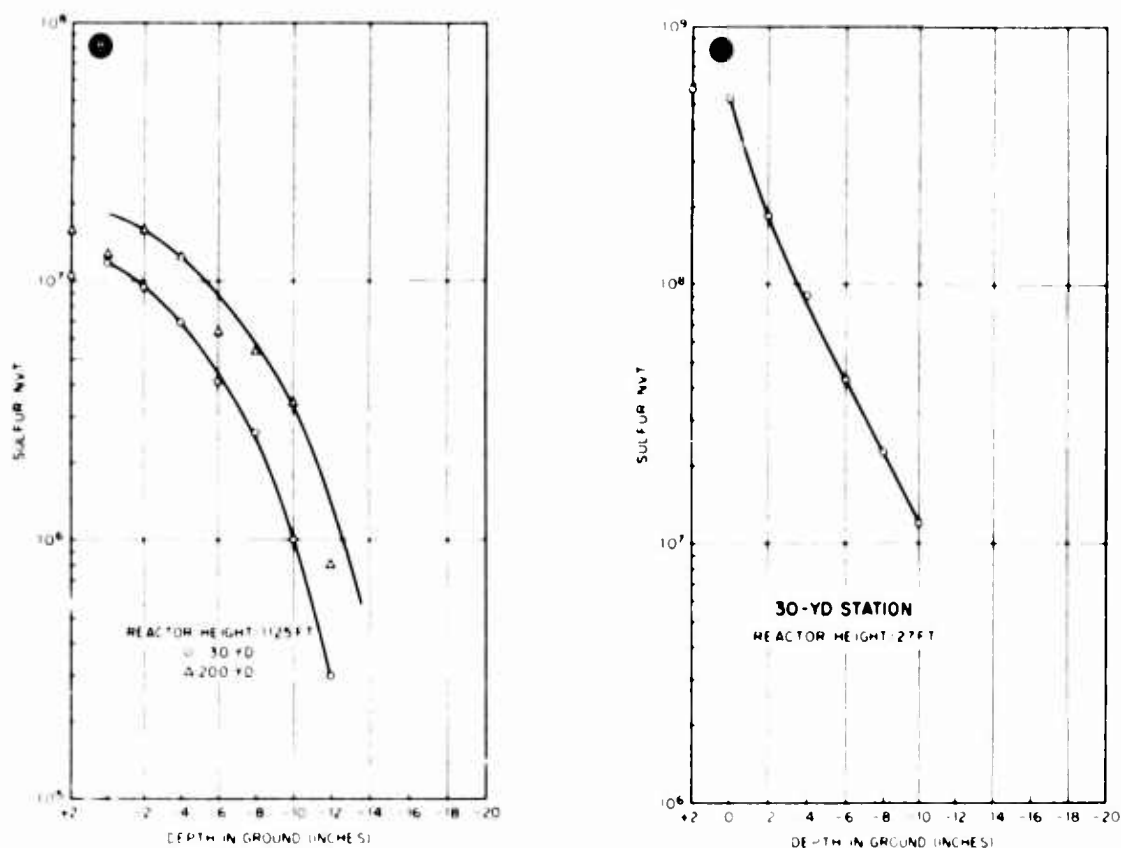


Fig. 3.14—Sulfur neutron activation. These curves give the relative activation in sulfur due to the (n,p) reaction. The ordinates are proportional to the neutron flux above about 3 Mev. Part A gives the relative surface flux vs. distance from the base of the tower for a reactor height of 1125 ft. The marked flux depression at the 30-yd station is attributed to attenuation by the tower. Parts B and C give the sulfur activation in the ground for three different geometries. Data were taken at 2 in. above the ground at each station.

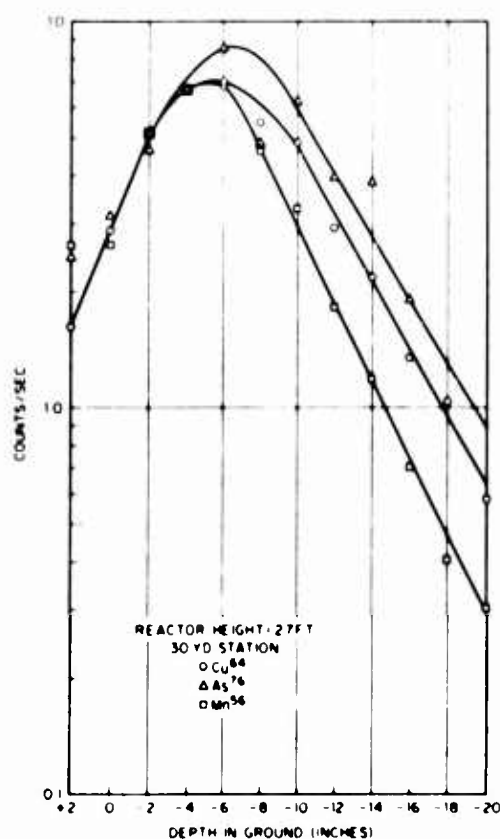


Fig. 3.15—Activation of manganese, copper, and arsenic. This curve shows the relative distributions with depth of the ^{56}Mn , ^{64}Cu , and ^{76}As induced by (n,γ) reactions in samples of the respective elements. The differences in shapes of the curves are attributed to the different energy variations of the activation cross sections.

CIVIL EFFECTS TEST OPERATIONS REPORT SERIES (CEX)

Through its Division of Biology and Medicine and Civil Effects Test Operations Office, the Atomic Energy Commission conducts certain technical tests, exercises, surveys, and research directed primarily toward practical applications of nuclear effects information and toward encouraging better technical, professional, and public understanding and utilization of the vast body of facts useful in the design of countermeasures against weapons effects. The activities carried out in these studies do not require nuclear detonations.

A complete listing of all the studies now underway is impossible in the space available here. However, the following is a list of all reports available from studies that have been completed. All reports listed are available at the prices indicated from the Clearinghouse for Federal Scientific and Technical Information, U. S. Department of Commerce, Springfield, Va.

- CEX-57-1, The Radiological Assessment and Recovery of Contaminated Areas, C. F. Miller, 1960, \$0.75.
- CEX-58-1, Experimental Evaluation of the Radiation Protection Afforded by Residential Structures Against Distributed Sources, J. A. Auxier, J. O. Buchanan, C. Eisenhauer, and H. F. Menker, 1959, \$2.75.
- CEX-58-2, The Scattering of Thermal Radiation into Open Underground Shelters, T. P. Davis, N. D. Miller, J. S. Fly, J. A. Basso, and H. E. Pearce, 1959, \$0.75.
- CEX-58-7, AEC Group Shelter, AEC Facilities Division, Holmes & Narver, Inc., 1960, \$0.50.
- CEX-58-8, Comparative Nuclear Effects of Biomedical Interest, C. S. White, I. G. Bowen, D. R. Richmond, and R. L. Corshie, 1961, \$1.00.
- CEX-58-9, A Model Designed to Predict the Motion of Objects Translated by Classical Blast Waves, I. G. Bowen, R. W. Albright, E. R. Fletcher, and C. S. White, 1961, \$1.25.
- CEX-59-1, An Experimental Evaluation of the Radiation Protection Afforded by a Large Modern Concrete Office Building, J. F. Butter, Jr., A. L. Kaplan, and E. T. Clarke, 1960, \$0.60.
- CEX-59-4, Aerial Radiological Monitoring System, I. Theoretical Analysis, Design, and Operation of a Revised System, R. F. Merian, J. G. Lackey, and J. E. Hand, 1961, \$1.25.
- CEX-59-4 (P. II), Aerial Radiological Monitoring System, Part II: Performance, Calibration, and Operational Check-out of the LG&G Arms-II Revised System, J. E. Hand, R. R. Gurlough, and H. M. Borella, 1962, \$1.50.
- CEX-59-4 (P. III), Aerial Radiological Monitoring System, Part III: Electronic Processing of ARMS-II Data, J. E. Hand and H. M. Borella, 1963, \$1.00.
- CEX-59-7 (P. I), Experimental Radiation Measurements in Conventional Structures, Part I: Comparison of Measurements in Above-ground and Below-ground structures from Simulated and Actual Fallout Radiation, Z. G. Burson, 1964, \$1.50.
- CEX-59-7C, Methods and Techniques of Fallout Studies Using a Particulate Simulant, W. Lee and H. Borella, 1962, \$0.50.
- CEX-59-13, Experimental Evaluation of the Radiation Protection Afforded by Typical Oak Ridge Homes Against Distributed Sources, T. D. Strickler and J. A. Auxier, 1960, \$0.50.
- CEX-59-14, Determinations of Aerodynamic Drag Parameters of Small Irregular Objects by Means of Drop Tests, I. P. Fletcher, R. W. Albright, A. C. Goldizen, and I. G. Bowen, 1961, \$1.75.
- CEX-60-1, Evaluation of the Fallout Protection Afforded by Brookhaven National Laboratory Medical Research Center, H. Borella, Z. Burson, and J. Jacobvitch, 1961, \$1.75.
- CEX-60-3, Extended and Point-source Radiometric Program, F. J. Davis and P. W. Reinhardt, 1962, \$1.50.
- CEX-60-5, Experimental Evaluation of the Fallout-radiation Protection Afforded by a Southwestern Residence, Z. Burson, D. Parry, and H. Borella, 1962, \$0.50.
- CEX-60-6, Experimental Evaluation of the Radiation Protection Provided by an Earth-covered Shelter, Z. Burson and H. Borella, 1962, \$1.00.
- CEX-61-1 (Prelim.), Gamma Radiation at the Air-Ground Interface, K. O'Brien and J. E. McLaughlin, Jr., 1963.
- CEX-61-4, Experimental Evaluation of the Fallout-radiation Protection Provided by Selected Structures in the Los Angeles Area, Z. G. Burson, 1963, \$2.25.
- CEX-62-01, Technical Concept—Operation BREN, J. A. Auxier, F. W. Sanders, F. F. Haywood, J. H. Thorngate, and J. S. Cheka, 1962, \$0.50.
- CEX-62-02, Operation Plan and Hazards Report—Operation BREN, F. W. Sanders, F. F. Haywood, M. I. Lundin, L. W. Gilley, J. S. Cheka, and D. R. Word, 1962, \$2.25.
- CEX-62-03, General Correlative Studies—Operation BREN, J. A. Auxier, F. F. Haywood, and L. W. Gilley, 1963, \$1.00.
- CEX-62-2, Nuclear Bomb Effects Computer (Including Slide-rule Design and Curve Fits for Weapons Effects), E. R. Fletcher, R. W. Albright, R. F. D. Perrett, Mary E. Franklin, I. G. Bowen, and C. S. White, 1963, \$1.00.
- CEX-62-11, Distribution of Weapons Radiation in Japanese Residential Structures, J. S. Cheka, F. W. Sanders, T. D. Jones, and W. H. Shipnough, 1963, \$1.00.
- CEX-62-14, An Experimental Investigation of the Spatial Distribution of Dose in an Air-over-ground Geometry, F. F. Haywood, J. A. Auxier, and E. T. Loy, 1964, \$1.00.
- CEX-62-81 (Prelim.), Ground Roughness Effects on the Energy and Angular Distribution of Gamma Radiation from Fallout, C. M. Huddleston, Z. G. Burson, R. M. Kinkaid, and Q. G. Klinger, 1963, \$1.25.
- CEX-63-3, Barrier Attenuation of Air-scattered Gamma Radiation, Z. G. Burson and R. L. Summers, 1965, \$1.00.
- CEX-63-7, A Comparative Analysis of Some of the Immediate Environmental Effects at Hiroshima and Nagasaki, C. S. White, I. G. Bowen, and D. R. Richmond, 1964, \$2.00.
- CEX-63-11, Mobile Radiological Measuring Unit: Description and Operating Information, Z. G. Burson, R. L. Summers, and J. T. Brashears, 1965, \$1.00.
- CEX-64-3, Ichiban—The Dosimetry Program for Nuclear Bomb Survivors of Hiroshima and Nagasaki—A Status Report as of April 1, 1964, J. A. Auxier, 1964, \$0.50.
- CEX-65-02, Technical Concept—Operation HENRE, S. F. Haywood and J. A. Auxier, 1965, \$1.00.